Nonlinear Optics: Materials, Fundamentals and Applications Topical Meeting and Tabletop Exhibit

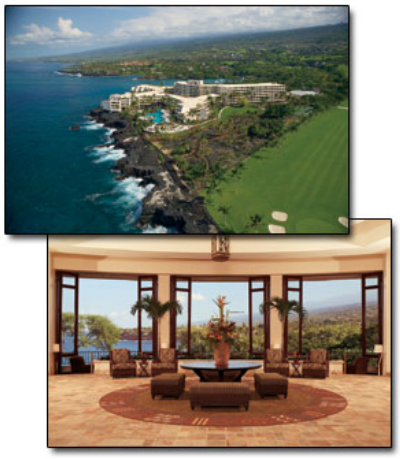

July 30–August 3, 2007
Sheraton Keauhou Bay Resort & Spa Kona, Hawaii

Postdeadline Paper Submission Deadline: June 28, 2007 at 12:00 p.m. noon EDT (16.00 GMT)
Hotel Reservation Deadline: July 6, 2007
Pre-Registration Deadline: July 5, 2007

Meeting Chairs

George Stegeman, *Univ. of Central Florida, USA,* General Chair
Antoinette Taylor, *Los Alamos Natl. Lab, USA,* General Chair
Martin Fejer, *Stanford Univ., USA,* Program Chair
Alexander Gaeta, *Cornell Univ., USA,* Program Chair

Support Provided By:

Swamp Optics

Taylor & Francis

About NLO

July 30–August 3, 2007

Nonlinear optical phenomena is being studied and applied over a wide range of powers, from picowatts to petawatts, and over broad spectral regimes, from mid-infrared to X-rays. The purpose of this meeting is to provide an international forum for discussion of all aspects of nonlinear optics, including new phenomena, novel devices, advanced materials and applications.

Important Dates:

OSA is now accepting POSTDEADLINE papers for Nonlinear Optics: Materials, Fundamentals and Application 2007. The deadline for the 35-word abstract and 3-page summary is June 28, 2007, 12:00 p.m. noon EDT (16.00 GMT).

Hotel Reservation Deadline: July 6, 2007
Pre-Registration Deadline: July 5, 2007

Meeting Topics to Be Considered

The topics to be considered in the main program will include (but not be limited to):

- Fundamental studies and new concepts
- Quantum optics, computation and communication
- Solitons and nonlinear propagation
- Ultrafast phenomena and techniques
- Surface, interface and nanostructure nonlinearities
- Microcavity and microstructure phenomena
- High intensity and relativistic nonlinear optics
- Slow light
- Coherent control
- Novel lasers and frequency converters
- Nonlinear materials
- Atoms, molecules and condensates
- Semiconductors
- Nanostructures
- Organics
- Photonic bandgap structures
- Fibers and waveguides
- Photorefractives
- Applications
- Lasers and amplifiers
- Frequency converters
- Optical communications
- Photonic switching
- Ultrafast measurement
- Frequency combs and optical clocks
- THz generation, spectroscopy and imaging
- Materials processing
- Optical storage

Program Committee

General Chairs

George Stegeman, *Univ. of Central Florida, USA*
Antoinette Taylor, *Los Alamos Natl. Lab, USA*

Program Chairs

Martin Fejer, *Stanford Univ., USA*
Alexander Gaeta, *Cornell Univ., USA*

Committee Members

Gaetano Assanto, *Univ. degli Studi Roma, Italy*
Andrius Baltuska, *Technische Univ. Wien, Austria*
Steven Cundiff, *NIST, USA*
Benjamin Eggleton, *Univ. of Sydney, Australia*
Jason Fleischer, *Princeton Univ., USA*
Daniel Gauthier, *Duke Univ., USA*
James Glownia, *Los Alamos Natl. Labs, USA*
Richard Haight, *IBM T.J. Watson Res. Ctr., USA*
Joseph Haus, *Univ. of Dayton, USA*
Fatih Ilday, *Bilkent Univ., Turkey*
Martti Kauranen, *Tampereen Teknillinen Korkeakoulu, Finland*
Barry Luther-Davies, *Australian Natl. Univ., Australia*
Daniel Mittleman, *Rice Univ., USA*
Stephen Rand, *Univ. of Michigan, USA*
Takunori Taira, *Inst. for Molecular Science, Japan*
Yurii Vlasov, *IBM TJ Watson Res. Ctr., USA*
Andrew Weiner, *Purdue Univ., USA*
Herbert Winful, *Univ. of Michigan, USA*
Aleksei Zheltikov, *Moscow State Univ., Russian Federation*

Nonlinear Optics (NLO) Topical Meeting & Tabletop Exhibit

Sheraton Keauhou Bay Resort & Spa ◆ Kona, Hawaii USA

July 30 – August 3, 2007

E X H I B I T O R S

Altos Photonics
201 S. Wallace, Suite B2C
Bozeman, MT
☎ 406.581.4662
🖷 909.363.8637
sales@altosphotonics.com
www.altosphotonics.com
Altos Photonics offers femtosecond, mode locked, and Q-switched lasers and tunable systems for research and industrial customers. Additional products include non-linear crystals (BBO, KTP, ZGP, KYW, KGW, etc), optical mounts, USB-controlled stages, and other related products. Altos Photonics sells and services products from EKSPLA, EKSMA, Light Conversion & Standa.

Del Mar Photonics
4119 Twilight Ridge
San Diego, CA 92130
☎ 858.876.3133
🖷 858.630.2376
sales@dmphotonics.com
www.dmphotonics.com
Manufacturer of femtosecond photonics products for scientific and industrial applications. Product portfolio includes ultrafast laser oscillators and amplifiers based on Ti:Sapphire, Cr:Forsterite, Er. and Yb. doped fiber, supercontinuum sources, table top multi terawatt systems; variety of measurement tools such as autocorrelators, SPIDER, cross-correlator and ultrafast dynamic measurement systems. Femtosecond systems for multiphoton imaging, nanophotonics, micromachining, terahertz spectroscopy, plasma and high-energy x-ray generation and other areas.

Swamp Optics, LLC
6300 Powers Ferry Rd #600-345
Atlanta, GA 30339-2919
☎ 404.547.9267
🖷 +1 866.855.4518
Linda.Trebino@SwampOptics.com
www.swampoptics.com
Optics offers inexpensive and easy-to-use devices for measuring ultrashort laser pulses in real time. Awards include 2004 Circle of Excellence and 2003 R&D100 for GRENOUILLE, which yield the most complete measurement of ultrashort pulses available, including the beam spatial profile and spatio-temporal distortions (spatial chirp and pulse-front tilt).

(see other side for more)

Laser Focus World

c/o PennWell Corporation
98 Spit Brook Rd.
Nashua, NH 03062
☎ 603.891.0123
🖷 603.891.0574
www.laserfocusworld.com

Laser Focus World is a monthly magazine for engineers, researchers, scientists and professionals providing comprehensive global coverage of optoelectronic technology and markets. It offers greater technical depth than any other publication in the field and keeps readers abreast of advances and trends in optoelectronics – lasers, fiberoptics, optical software and computing, imaging and instrumentation.

Photonics Spectra

2 South Street
Berkshire Common
Pittsfield, MA 01201
☎ 413.499.0514
🖷 413.442.3180
photonics@laurin.com
www.Photonics.com/spectra

Photonics Spectra is the leading photonics magazine serving industries that use photonic technology: lasers, imaging, fiber optics, optics, electro-optics, and photonic component manufacturing. It presents the latest news articles and in-depth reports on photonics technology. It is distributed free to those who use or apply photonics.

Special Events

Poster Session

Wednesday, August 1 * 3:30 p.m. – 6:00 p.m. * Keauhou Ballroom 1
Over 30 posters will be presented and light refreshments will be served.

Conference Luau

Wednesday, August 1 * 6:00 p.m. – 10:00 p.m. * Hawaii Lawn & Crystal Blue Point
Join your colleagues for a traditional Hawaiian Luau. The cost of the luau is included in the price of registration for technical registrants. Guest tickets may be purchased at the registration desk by 12:00 p.m. on Monday, July 30.

Invited Speakers

Plenary

MA1, **Quantum Control with Classical Pulses and Photons,** *Yaron Silberberg; Weizmann Inst. of Science, Israel.*

ThA1, **Clocks, Combs and Optical Arbitrary-Waveform Generators,** *Erich Ippen; MIT, USA.*

TuA1, **Opportunities in Nonlinear Optical Spectroscopy,** *Yuen-Ron Shen; Physics Dept., Univ. of California at Berkeley, USA.*

Invited Speakers

WD2, **Photonic-Crystal Nanocavities and Their Applications,** *Susumu Noda; Kyoto Univ., Japan.*

WD3, **Nonlinear Optical Processes in Photonic Crystal Microcavities**, *Jelena Vuckovic; Stanford Univ., USA.*

ThA2 **Advances in Femtosecond Fiber Lasers**, *Frank Wise; Cornell Univ., USA.*

ThB1, **Attosecond X-Ray Photonics: All-Optical Quasi-Phase Matching for High Harmonic Generation**, *Oren Cohen, Xiaoshi Zhang, Amy Lytle, Henry Kapteyn, Margaret Murnane; JILA, Univ. of Colorado, USA.*

ThB3, **Xe Plasma Generated by a Cavity Enhanced Yb-Similariton Laser Based Fiber Frequency Comb**, *Ingmar Hartl[1], A. Marcinkevicius[1], M. E. Fermann[1], T. R. Schibli[2], D. D. Hudson[2], D. C. Yost[2], J. Ye[2]; [1]IMRA America, Inc., USA, [2]NIST and Univ. of Colorado, USA.*

ThB5, **Compact 0.56 Petawatt Laser System Based on OPCPA**, *Efim A. Khazanov, V. V. Lozhkarev, G. I. Friedman, V. N. Ginzberg, E. V. Katin, A. V. Kirsanov, G. A. Luchinin, A. N. Mal'shakov, M. A. Matryanov, O/V. Palashov, A. K. Poteomkin, A. M. Sergeev, A. A. Shaykin, I. V. Yakovlev; Inst. of Applied Physics, Russian Federation.*

FA1, **High Intensity Fiber Lasers: From EUV Lithography to Hard X-Ray Generation**, *Almantas Galvanauskas; Univ. of Michigan, USA.*

FA6, **Nonlinear Optical Microscopy: From Imaging Molecular Dynamics to Blood Flow in Living Systems,** *Jeffrey Squier[1], Dawn Schafer[1], Rob Applegate[1], Ramon Carriles[1], Wafa Amir[1], David Marr[1], Ralph Jimenez[2], Emily Gibson[1], Michiel Muller[3]; [1]Colorado School of Mines, USA, [2]Univ. of Colorado, USA, [3]Univ. of Amsterdam, The Netherlands.*

FB1, **Nonlinear Opto-Mechanics Using Radiation Pressure in Micro-Cavities**, *Kerry Vahala[1], Tal Carmon[1], Tobias Kippenberg[2], Mani Hosein Zadeh[1]; [1]Caltech, USA, [2]Max Planck Inst. fur Quantenoptik, Germany.*

FB3, **Optical Frequency Comb Generation from a Monolithic Micro-Resonator via the Kerr Nonlinearity**, *Pascal Del'Haye, Albert Schliesser, Tobias Wilken, Ronald Holzwarth, Tobias Kippenberg; Max-Planck-Inst. for Quantum Optics, Germany.*

Program Agenda

	Keauhou 2 Ballroom	Keauhou 3 Ballroom
Sunday, July 29, 2007		
2:00 p.m. – 6:00 p.m.	Registration Open (Keauhou Ballroom Foyer)	
Monday, July 30, 2007		
7:00 a.m. – 12:30 p.m.	Registration Open (Keauhou Ballroom Foyer)	
8:00 a.m. – 10:00 a.m.	MA • Plenary I	
10:00 a.m. – 10:30 a.m.	Coffee Break (Keauhou Ballroom Foyer)	
10:00 a.m. – 12:30 p.m.	Exhibits (Keauhou Ballroom Foyer)	
10:30 a.m. – 12:30 p.m.	MB • Ultrafast Nonlinear Optics	MC • Nonlinear Optics in Novel Structures I
7:30 p.m. – 9:30 p.m.	MD • Nonlinear Optics in Novel Structures II	
Tuesday, July 31, 2007		
7:30 a.m. – 12:30 p.m.	Registration Open (Keauhou Ballroom Foyer)	
8:00 a.m. – 10:00 a.m.	TuA • Plenary II	
10:00 a.m. – 10:30 a.m.	Coffee Break (Keauhou Ballroom Foyer)	
10:00 a.m. – 12:30 p.m.	Exhibits (Keauhou Ballroom Foyer)	
10:30 a.m. – 12:00 p.m.	TuB • Nonlinear and Terahertz Spectroscopy	TuC • Nonlinear Propagation Dynamics
7:30 p.m. – 9:30 p.m.	TuD • Nonlinear Optics in Si Nanostructures	
Wednesday, August 1, 2007		
7:30 a.m. – 6:00 p.m.	Registration Open (Keauhou Ballroom Foyer)	
8:00 a.m. – 10:00 a.m.	WA • Metamaterials	
10:00 a.m. – 10:30 a.m.	Coffee Break (Keauhou Ballroom Foyer)	
10:00 a.m. – 12:30 p.m.	Exhibits (Keauhou Ballroom Foyer)	
10:30 a.m. – 12:30 p.m.	WB • Nonlinear Processes in Guided-Wave Geometries	WC • Nonlinear Optical Materials (ends at 12:45 p.m.)
2:00 p.m. – 3:30 p.m.	WD • Photonic Crystal Microcavities	
2:00 p.m. – 5:30 p.m.	Exhibits (Keauhou Ballroom Foyer)	
3:30 p.m. – 6:00 p.m.	WE • NLO Poster Session (Keauhou Ballroom 1)	
6:00 p.m. – 8:00 p.m.	Conference Luau (Hawaii Lawn & Crystal Blue Point)	
Thursday, August 2, 2007		
7:30 a.m. – 12:30 p.m.	Registration Open (Keauhou Ballroom Foyer)	
8:00 a.m. – 10:00 a.m.		ThA • Plenary III
10:00 a.m. – 10:30 a.m.	Coffee Break (Keauhou Ballroom Foyer)	
10:00 a.m. – 12:30 p.m.	Exhibits (Keauhou Ballroom Foyer)	
10:30 a.m. – 12:30 p.m.		ThB • Attosecond and X-Ray Generation
7:30 p.m. – 9:30 p.m.		ThC • Postdeadline Session
Friday, August 3, 2007		
7:30 a.m. – 12:30 p.m.	Registration Open (Keauhou Ballroom Foyer)	
8:00 a.m. – 10:00 a.m.		FA • Novel Sources and Applications
10:00 a.m. – 10:30 a.m.	Coffee Break (Keauhou Ballroom Foyer)	
10:00 a.m. – 12:30 p.m.	Exhibits (Keauhou Ballroom Foyer)	
10:30 a.m. – 12:30 p.m.		FB • Nonlinear Optics in Microresonators

Nonlinear Optics: Materials, Fundamentals and Applications 2007 Abstracts

•Sunday, July 29, 2007•

Keauhou Ballroom Foyer
2:00 p.m.–6:00 p.m.
Registration Open

•Monday, July 30, 2007•

Keauhou Ballroom Foyer
7:00 a.m.–12:30 p.m.
Registration Open

MA • Plenary I

Keauhou 2 Ballroom
8:00 a.m.–10:00 a.m.
MA • Plenary I
Martin M. Fejer; Stanford Univ., USA, Presider

MA1 • 8:00 a.m. Plenary
Quantum Control with Classical Pulses and Photons, *Yaron Silberberg; Weizmann Inst. of Science, Israel.* No abstract available.

MA2 • 9:00 a.m. Invited
Nonlinear Optics with Biphotons, *Stephen E. Harris; Stanford Univ., USA.* No abstract available.

MA3 • 9:30 a.m.
High-Efficiency Source of a Three-Photon W State and Its Full Characterization Using Quantum State Tomography, *Takayoshi Kobayashi[1,2,3,4], Hideharu Mikami[1,2], Yongmin Li[1,2], Kyosuke Fukuoka[1,2]; [1]Dept. of Physics, Graduate School of Science, Univ. of Tokyo, Japan, [2]Core Res. for Evolutional Science and Technology, Japan Science and Technology Agency, Japan, [3]Dept. of Applied Physics and Inst. of Laser Res., the Univ. of Electro-Communications, Japan, [4]Dept. of Electrophysics, Advanced Ultrafast Laser Ctr., Natl. Chiao-Tung Univ., Taiwan.* We proposed and demonstrated a high-efficiency generation scheme of the three-photon polarization-entangled *W* state, which is one of two typical three-qubit entangled states. The obtained state was well characterized using a method of quantum-state tomography.

MA4 • 9:45 a.m.
All-Fiber Telecom-Band Correlated Photon-Pair Source for 10 GHz Quantum Applications, *Chuang Liang, Matthew Shin, Kim F. Lee, Jun Chen, Prem Kumar; Northwestern Univ., USA.* We demonstrate a 9.95 GHz operated all-fiber source for generating telecom-band correlated photon pairs. Greater than 19 coincidences to accidentals ratio is observed with raw photon-counting data, i.e., without making any post-measurement corrections.

Keauhou Ballroom Foyer
10:00 a.m.–10:30 a.m.
Coffee Break

Keauhou Ballroom Foyer
10:00 a.m. – 12:30 p.m.
Exhibits

MB • Ultrafast Nonlinear Optics

Keauhou 2 Ballroom
10:30 a.m.–12:30 p.m.
MB • Ultrafast Nonlinear Optics
Erich Ippen; MIT, USA, Presider

MB1 • 10:30 a.m. Invited
Carrier-Envelope Phase Controlled Ultrashort Light Pulses for Nonlinear Optics, *Franz X. Kaertner, A. Benedick, J. Birge, M. Sander; MIT, USA.* Broadband Ti:sapphire lasers based on double-chirped mirror pairs deliver 5fs-pulses with octave-spanning spectra for direct carrier-envelope phase locking. Further development of these lasers in terms of higher repetition rates and broader output spectra is discussed.

MB2 • 11:00 a.m.
Fourier-Synthesis of Phase Coherent Raman Sidebands and Full Characterization of the Temporal Waveform, *Masayuki Katsuragawa[1,2], Takashi Onose[1,2], Takayuki Suzuki[1], Kazuhiko Misawa[3]; [1]Univ. of Electro-Communications, Japan, [2]PRESTO, JST, Japan, [3]Tokyo Univ. of Agriculture and Technology, Japan.* We generate a train of highly-stable ultrashort-pulses with a repetition-rate of 10.6 THz by synthesizing phase-coherent rotational-Raman-sidebands in parahydrogen. We also show full characterization of its temporal waveform based on a frequency-resolved-optical-gating method.

MB3 • 11:15 a.m.
Enhancement of High-Harmonic Generation by Laser-Induced Cluster Vibration and Its Application to Diagnosis of Clusters, *Yen-Mu Chen[1], Ming-Yu Hsu[2], Jiunn-Yuan Lin[2], Yi-Hsian Hsieh[3], Jyhpyng Wang[3], Szu-yuan Chen[3]; [1]Dept. of Physics, Natl. Taiwan Univ., Taiwan, [2]Dept. of Physics, Natl. Chung Cheng Univ., Taiwan, [3]Inst. of Atomic and Molecular Sciences, Academia Sinica, Taiwan.* Enhancement of high-harmonic-generation efficiency of a cluster jet by an order of magnitude is achieved at adequate prepulse-pump delays. This effect also allows characterization of the size and vibration dynamics of atom clusters.

MB4 • 11:30 a.m.
Ultrafast Carrier Dynamics in Semiconductor Nanowires, *Rohit P. Prasankumar[1], George T. Wang[2], Teresa Clement[3], Sukgeun Choi[1], Samuel T. Picraux[1,3], Antoinette J. Taylor[1]; [1]Los Alamos Natl. Lab, USA, [2]Sandia Natl. Labs, USA, [3]Arizona State Univ., USA.* Time-resolved measurements of carrier dynamics in Ge and GaN nanowires reveal that carrier relaxation in these systems is governed by surface states and defects. This has significant implications for nanowire-based devices in photonics and thermoelectrics.

MB5 • 11:45 a.m.
Simple Measurement of Ultrashort Pulses, *Rick Trebino, Dongjoo Lee, Selcuk Akturk, Pablo Gabolde, Xuan Liu, Pamela Bowlan; Georgia Tech, USA.* We demonstrate and simulate ultrasimple, alignment-free, single-shot devices for measuring broadband ultrashort pulses. We also present a simple single-shot method for measuring the complete spatio-temporal pulse field, for measuring nonlinear-optical effects, such as continuum generation.

MB6 • 12:00 p.m.
Background-Free Collinear Autocorrelation and Frequency-Resolved Optical Gating Using Mode Multiplexing and Demultiplexing in Reverse-Proton-Exchange Aperiodically Poled Lithium Niobate Waveguides, *Carsten Langrock, Martin M. Fejer; Stanford Univ., USA.* We use mode multiplexing in periodically poled lithium niobate waveguides to characterize picosecond optical pulses in a collinear but background-free way using autocorrelation and second harmonic frequency resolved optical gating.

MB7 • 12:15 p.m.
Synchronously Pumped Femtosecond Cascaded Optical Parametric Oscillation and Second Harmonic Generation in Periodically Poled MgO:SLN, *Felix Rüebel, Peter Haag, Johannes A. L'huillier; Technische Univ. Kaiserslautern, Germany.* We report on a synchronously pumped femtosecond cascaded OPO/SHG process in a single MgO:PPLN with an average output power of 160 mW at 583 nm pumped with 1.4 W at 780 nm.

Keauhou Ballroom Foyer
10:00 a.m.–10:30 a.m.
Coffee Break

Keauhou Ballroom Foyer
10:00 a.m. – 12:30 p.m.
Exhibits

MC • Nonlinear Optics in Novel Structures I

Keauhou 3 Ballroom
10:30 a.m.– 12:30 p.m.
MC • Nonlinear Optics in Novel Structures I
Shanhui Fan; Stanford Univ., USA, Presider

MC1 • 10:30 a.m.
Origin of Second-Harmonic Generation from Metal Nanodimers with a Nanogap, *Martti Kauranen[1], Hannu Husu[1], Brian K. Canfield[1], Janne Laukkanen[2], Benfeng Bai[2], Markku Kuittinen[2], Jari Turunen[2]; [1]Tampere Univ. of Technology, Finland, [2]Univ. of Joensuu, Finland.* Second-harmonic generation from noncentrosymmetric gold nanodimers with a nanogap is not dominated by field enhancement in the gap. Instead, polarization conversion in the local field and its asymmetric distribution around the dimer perimeter dominate.

MC2 • 10:45 a.m.
Quasi-Phase-Matching with Simultaneously Electronic and Magnetic Nonlinear Response in Metamaterials, *Simin Feng, Klaus Halterman; Naval Air Warfare Ctr., USA.* Condition of quasi-phase matching of parametric processes is investigated in multilayer metamaterials consisting of nonlinear positive-index and negative-index medium. The positive component has nonlinear electronic response, whereas the negative component has nonlinear magnetic response.

MC3 • 11:00 a.m. Invited
Optical Second Harmonic Generation from Metallic Nanostructures, *Pierre-François Brevet; Lab de Spectrométrie Ionique et Moléculaire, Univ. Claude Bernard Lyon 1, France.* Optical second harmonic response from randomly distributed small gold and silver metallic particles the diameter of which ranges from ten to over 100 nanometers has been investigated in solution with the technique of Hyper-Rayleigh Scattering.

MC4 • 11:30 a.m.
Optical Nonlinearities and Multiexciton Statistics in Semiconductor Nanocrystals in the Regime of Carrier Multiplication, *Victor I. Klimov, Richard D. Schaller; Los Alamos Natl. Lab, USA.* We analyze band-edge optical nonlinearities and carrier-population statistics in PbSe nanocrystals in the regime when high-order multiexcitons with multiplicity up to seven are generated via carrier multiplication by single absorbed photons.

MC5 • 11:45 a.m.
Nonlinear Refraction of Semiconductor Quantum Dots Using Single Wavelength and White-Light Continuum Z-Scan, *Lazaro A. Padilha, Gero Nootz, Mihaela Balu, David J. Hagan, Eric W. Van Stryland; CREOL, Univ. of Central Florida, USA.* The nonlinear refractive index is measured in semiconductor quantum-dots using white light continuum Z-scan, which can measure nonlinear refraction as small as 10^{-16}cm^2/GW. The magnitude of the nonlinearity decreases for smaller quantum-dots.

MC6 • 12:00 p.m.
Opto-Mechanical Modal Spectroscopy: Opto-Excited Vibrations of a Micron-Scale On-Chip Resonator, *Tal Carmon, Kerry J. Vahala; Caltech, USA.* Radiation-pressure is used to excite vibrational modes of an optical micro-cavity at GHz rates. Many spectral lines associated with high-order vibrational modes are measured. Perturbation of the cavity geometry is measured to induce spectral-lines splitting.

MC7 • 12:15 p.m.
Two-Photon Emission from Semiconductor Device, *Alex Hayat, Meir Orenstein; Dept. of Electrical Engineering, Technion, Israel.* We report experimental observations of spontaneous two-photon emission from semiconductors. The wide-band two-photon emission intensity was 4 orders of magnitude lower than the fundamental emission and blue-shifted due to significant k-dependence of the matrix element.

MD • Nonlinear Optics in Novel Structures II

Keauhou 2 Ballroom
7:30 p.m.–9:30 p.m.
MD • Nonlinear Optics in Novel Structures II
Michal Lipson; Cornell Univ., USA, Presider

MD1 • 7:30 p.m. Invited
Classical and Quantum Nonlinear Optics in Photonic Crystals, *Shanhui Fan; Stanford Univ., USA.* We show that photonic crystals can be used to control self-focusing and to induce strong photon-photon interaction at a few-photon level.

MD2 • 8:00 p.m.
SHG with Self-Phasematching in a Semiconductor Microcavity, *Alex Hayat, Meir Orenstein; Dept. of Electrical Engineering, Technion, Israel.* We fabricated semiconductor microcavities for self-phase-matched nonlinear optics. The measured efficiency shows a strong maximum at cavity resonance due to cavity enhanced pump input power and dispersion-induced wavelength-detuning effect on the mode overlap.

MD3 • 8:15 p.m. Invited

Enabling Optical Nonlinearities at Very Low Power Levels, *Marin Soljacic; MIT, USA.* We present a few schemes for enhancing all-optical nonlinearities. Among them, we show how Purcell effect can be used to tailor optical nonlinearities.

MD4 • 8:45 p.m.

Extreme Nonlinear Phase Shift in Self-Pulsating Laser Diodes, *Makoto Ohta[1,2], Masaru Kuramoto[2], Masao Ikeda[1,2], Hiroyuki Yokoyama[1]; [1]Tohoku Univ., Japan, [2]Sony Corp., Japan.* We observed strong self-phase-modulation of over 20π inside self-pulsating laser diodes. We found that this phenomenon plays a crucial role in reducing noise when using a semiconductor laser to read information from an optical disk.

MD5 • 9:00 p.m. Invited

On the Uniqueness of Hollow-Core Photonic Band-Gap Fiber, *Karl Koch; Corning, Inc., USA.* The optical properties of hollow-core photonic band-gap fibers can differ from those of conventional optical fibers by many orders of magnitude. We review these optical properties and discuss their impact on applications.

•Tuesday, July 31, 2007•

Keauhou Ballroom Foyer
7:30 a.m.–12:30 p.m.
Registration Open

TuA • Plenary II

Keauhou 2 Ballroom
8:00 a.m.–10:00 a.m.
TuA • Plenary II
Antoinette J. Taylor; Los Alamos Natl. Lab, USA, Presider

TuA1 • 8:00 a.m. Plenary

Opportunities in Nonlinear Optical Spectroscopy, *Yuen-Ron Shen; Physics Dept., Univ. of California at Berkeley, USA.* No abstract available.

TuA2 • 9:00 a.m. Invited

Probing Exciton Coupling and Correlation in Semiconductors with Optical Two-Dimensional Fourier Transform Spectroscopy, *Xiaoqin Li[1], Tianhao Zhang[2], S. T. Cundiff[2]; [1]Univ. of Texas at Austin, USA, [2]JILA, Univ. of Colorado and NIST, USA.* We study many-body interactions between excitons in semiconductors by applying a new and powerful technique, optical two-dimensional Fourier transform spectroscopy.

TuA3 • 9:30 a.m. Invited

Photospin State Selectivity and Manipulation in Photonic Structures, *Christos Flytzanis; Ecole Normale Superieure de Paris, France.* Inclusion of nonlocality in constitutive relations in photonic cystals has important repercussions in polarization-state behaviour of electromagnetic modes.

Keauhou Ballroom Foyer
10:00 a.m.–10:30 a.m.
Coffee Break

Keauhou Ballroom Foyer
10:00 a.m.–12:30 p.m.
Exhibits

TuB • Nonlinear and Terahertz Spectroscopy

Keauhou 2 Ballroom
10:30 a.m.–12:00 p.m.
TuB • Nonlinear and Terahertz Spectroscopy
James Glownia; Los Alamos Natl. Lab, USA, Presider

TuB1 • 10:30 a.m.

Generation of Broadband Terahertz Pulses on a Metal Wire Waveguide via Optical Rectification, *Ajay Nahata[1], Hua Cao[2]; [1]Univ. of Utah, USA, [2]Univ. of South Florida, USA.* We demonstrate the generation of broadband terahertz pulses on a cylindrical metal wire via optical rectification in a poled polymer layer. Optical pulses are coupled onto the wire using a groove milled into the wire.

TuB2 • 10:45 a.m.

Split-Ring Resonator Enhanced Terahertz Antenna, *John F. O'Hara[1], Hou-Tong Chen[1], Antoinette J. Taylor[1], Richard D. Averitt[2], Willie J. Padilla[3]; [1]Los Alamos Natl. Lab, USA, [2]Boston Univ., USA, [3]Boston College, USA.* An electric split-ring resonator is used to enhance the performance of a photoconductive dipolar antenna based terahertz transmitter. Enhancement is observed near and limited to the resonant frequency of the electric split-ring resonator.

TuB3 • 11:00 a.m.

Symmetry Folding in the Azimuthal Angle Dependence of the Terahertz Radiation of (100) p-InAs under 1 Tesla Magnetic Field, *Elmer Estacio[1], Carlito Ponseca[2], Hisashi Sumikura[1], Hidetoshi Murakami[1], Shingo Ono[3], Romeric Pobre[4], Reuben Quiroga[4], Nobuhiko Sarukura[1], Masahiko Tani[1], Masanori Hangyo[1]; [1]Inst. of Laser Engineering, Osaka Univ., Japan, [2]Inst. for Molecular Science, Japan, [3]Nagoya Inst. of Technology, Japan, [4]Dept. of Physics, De La Salle Univ., Philippines.* Azimuthal angle dependence of the terahertz radiation of (100) p-type InAs under 1-T field is presented. Four-fold symmetry for p-polarized radiation emerged and the same is seen for the s-polarized radiation for the no-field case.

TuB4 • 11:15 a.m. Invited

Ultrafast Spectroscopy of Excitons and Phonons in Carbon Nanotubes, *Junichiro Kono; Rice Univ., USA.* No abstract available.

TuB5 • 11:45 a.m.

Influence of Intrinsic and Extrinsic Defects on the Recombination Behavior of Light-Induced Hole Polarons, *Bettina Schoke, Christoph Merschjann, Stefan Torbrügge, Mirco Imlau, Michael Rohlfing; Univ. of Osnabrueck, Germany.* The influence of intrinsic and extrinsic defects on small bound hole-polarons is investigated in $LiNbO_3$ and $KNbO_3$ via ESA spectroscopy. Intrinsic defects most probably change the polaron absorption, extrinsic defects affect the relaxation of hole-polarons.

Keauhou Ballroom Foyer
10:00 a.m.–10:30 a.m.
Coffee Break

Keauhou Ballroom Foyer
10:00 a.m.–12:30 p.m.
Exhibits

TuC • Nonlinear Propagation Dynamics

Keauhou 3 Ballroom
10:30 a.m.–12:30 p.m.
TuC • Nonlinear Propagation Dynamics
Daniel Gauthier; Duke Univ., USA, Presider

TuC1 • 10:30 a.m. **Invited**
Spatial-Spectral Shaping of Supercontinuum Radiation in Nonlinear Waveguide Arrays, *Dragomir N. Neshev; Australian Natl. Univ., Australia.* This talk presents the experimental realisation of simultaneous spatial-spectral shaping of beams with ultra-broad and supercontinuum spectral bandwidth in nonlinear waveguide arrays, revealing novel phenomena of light localization and formation of polychromatic gap solitons.

TuC2 • 11:00 a.m.
Discrete Spatial Surface Solitons at the Interface between Dissimilar Arrays, *Sergiy Suntsov[1], Konstantinos Makris[1], Demetrios Christodoulides[1], George Stegeman[1], Christian Rüter[2], Detlef Kip[2], Roberto Morandotti[3], Maïte Volatier[4], Vincent Aimez[4], Richard Ares[4], Haeyeon Yang[5], Gregory Salamo[5]; [1]College of Optics and Photonics, CREOL and FPCE, Univ. of Central Florida, USA, [2]Inst. of Physics and Physical Technologies, Clausthal Univ. of Technology, Germany, [3]Inst. Natl. de la Recherche Scientifique, Univ. du Quebec, Canada, [4]Ctr. de Recherche en Nanofabrication et en Nanocaractérisation, CRN[2], Univ. de Sherbrooke, Canada, [5]Physics Dept., Univ. of Arkansas, USA.* We have observed surface solitons guided by the interface between two dissimilar arrays of weakly coupled AlGaAs waveguides. Only one interface soliton was observed, different from the soliton families found between discrete and continuous media.

TuC3 • 11:15 a.m.
Self-Steepening of Ultrashort Optical Pulses without Self-Phase Modulation, *Jeffrey Moses[1], Boris A. Malomed[2], Frank W. Wise[1]; [1]Cornell Univ., USA, [2]Tel Aviv Univ., Israel.* A first optical manifestation of the Chen-Lee-Liu-type derivative nonlinear Schröedinger equation results in self-steepening of ultrashort pulses and shock formation without simultaneous self-phase modulation. Experiments verify theory.

TuC4 • 11:30 a.m.
All-Optical Plasma Turbulence, *Dmitry V. Dylov, Jason W. Fleischer; Princeton Univ., USA.* We consider an all-optical bump-on-tail instability. For weak nonlinearity, there is momentum transfer with no variation in intensity. Above a threshold, modulations appear. Borrowing plasma language, these represent weak and strong regimes of optical turbulence.

TuC5 • 11:45 a.m.
Nonlocal Explanation of Stationary and Nonstationary Regimes in Cascaded Pulse Compression, *Ole Bang[1], Morten Bache[1], Jeffrey Moses[2], Frank Wise[2]; [1]COM.DTU, Technical Univ. of Denmark, Denmark, [2]Dept. of Applied and Engineering Physics, Cornell Univ., USA.* We study pulse compression in quadratic materials and show that group-velocity mismatch creates two nonlocal oscillatory and localized regimes that describe nonstationary and stationary pulse compression. The theory is used to accurately predict the transition.

TuC6 • 12:00 p.m.
Collapse and Stability of Necklace Beams in Kerr Media, *Taylor D. Grow, Amiel A. Ishaaya, Luat T. Vuong, Alexander L. Gaeta; Cornell Univ., USA.* We experimentally investigate necklace beams in Kerr media. For powers greater than one critical power for self-focusing per bead, we observe a transition from collective behavior to independent collapse of each of the beads.

TuC7 • 12:15 p.m.
Nonlinear Terahertz Wave Photonics in Laser-Induced Air Plasma, *Jianming Dai, Xu Xie, X.-C. Zhang; Ctr. for Terahertz Res., Rensselaer Polytechnic Inst., USA.* We report the generation, manipulation, amplification and detection of THz waves in laser induced air plasma. Four-wave mixing is the main mechanism of THz wave photonics in plasma.

TuD • Nonlinear Optics in Si Nanostructures

Keauhou 2 Ballroom
7:30 p.m.–9:30 p.m.
TuD • Nonlinear Optics in Si Nanostructures
Presider to Be Announced

TuD1 • 7:30 p.m. **Invited**
All Optical Wavelength Conversion and Nonlinear Functions Enhanced in Ultra-Small Silicon Waveguides, *Koji Yamada[1], H. Fukuda[1], T. Wantanabe[1], T. Tsuchizawa[1], T. Tanabe[2], S. Itabashi[1]; [1]NTT Microsystem Integration Labs, Japan, [2]NTT Basic Res. Labs, Japan.* Efficient nonlinear functions, such as wavelength conversion and all-optical amplitude modulation, in silicon wire waveguides are demonstrated. Efficiencies of these functions are now reaching practical standards, and will be further improved by eliminating free-carrier absorption.

TuD2 • 8:00 p.m.
Study on Nonlinear Optical Property of Amorphous Silicon, *Kazuhiro Ikeda, Yaoming Shen, Yeshaiahu Fainman; Univ. of California at San Diego, USA.* Enhanced free carrier nonlinearity due to midgap localized states in amorphous silicon is measured and discussed. We also propose a new waveguide structure to utilize this material in practical devices.

TuD3 • 8:15 p.m. **Invited**
Nonlinear Optics in High Confinement Silicon Nanostructures, *Michal Lipson; Cornell Univ., USA.* No abstract available.

TuD4 • 8:45 p.m.
Broad-Band Continuous-Wave Four-Wave Mixing in Silicon Wire Waveguides, *Mark A. Foster, Reza Salem, David F. Geraghty, Amy C. Turner, Michal Lipson, Alexander L. Gaeta; Cornell Univ., USA.* We demonstrate continuous-wave four-wave mixing over an extremely broad bandwidth using dispersion-engineered silicon nanowaveguides, which allow for efficient wavelength conversion across four telecommunication bands from 1477 nm to 1672 nm.

TuD5 • 9:00 p.m. **Invited**
Nonlinear Quantum Optics in Rings and Other Things, *John Sipe; Univ. of Toronto, Canada.* No abstract available.

•Wednesday, August 1, 2007•

Keauhou Ballroom Foyer
7:30 a.m. – 6:00 p.m.
Registration Open

WA • Metamaterials

Keauhou 2 Ballroom
8:00 a.m.–10:00 a.m.
WA • Metamaterials
Presider to Be Announced

WA1 • 8:00 a.m. Invited

Nonlinearities in Negative Refractive Index Media, *Aref Chowdhury; Bell Labs, Alcatel-Lucent, USA.* We will review the progress made in the area of nonlinear phenomena and negative refractive index metamaterials. We will also discuss recent studies on susceptibility, wave-mixing and other nonlinear resonance properties of metamaterials.

WA2 • 8:30 a.m.

Liquid Crystalline Supra-Nonlinear Optical Metamaterials with Tunable Negative-, Zero- and Positive- Refractive Indices, *I. C. Khoo, A. Diaz, D. H. Kwon, D. H. Werner; Pennsylvania State Univ., USA.* We demonstrate by theory and experiments the feasibility of realizing liquid crystalline supra-nonlinear optical metamaterials with tunable negative-zero-positive refractive indices and nonlinear coefficient far exceeding 1 cm^2/W in the visible-infrared regime.

WA3 • 8:45 a.m. Invited

Negative Refraction and Electromagnetically Induced Chirality, *Susanne Yelin; Univ. of Connecticut, USA.* Negative refraction with minimal absorption obtained using quantum interference effects similar to electromagnetically induced transparency. Coupling a magnetic dipole transition coherently with an electric dipole transition leads to electromagnetically induced chirality, providing negative refraction.

WA4 • 9:15 a.m.

Left Handed Material at Optical Wavelength, *Byoung-Joon Seo[1], Tetsuya Ueda[2], Bart Bortnik[1], Tatsuo Itoh[1], Harold R. Fetterman[1]; [1]Univ. of California at Los Angeles, USA, [2]Kyoto Inst. of Technology, Japan.* We present a left-handed material (LHM) at optical wavelength. Our structure consists of polystyrene spheres on layers of metals. Measurement of LHM is discussed, suggesting that our structure has a negative refractive index near 470nm.

WA5 • 9:30 a.m. Invited

Nonlinear Pulse Propagation Effects in Metamaterials: Solitons, Gap Solitons, and the Influence of Phase Matching on Second Harmonic Generation, *Michael Scalora; US Army, USA.* We present evidence that a phase locking mechanism characterizes harmonic generation under phase mismatched conditions. The SH and TH signals display two peaks, a normal and a phase-locked component that phase-locks to the pump.

Keauhou Ballroom Foyer
10:00 a.m.–10:30 a.m.
Coffee Break

Keauhou Ballroom Foyer
10:00 a.m.–12:30 p.m.
Exhibits

WB • Nonlinear Processes in Guided-Wave Geometries

Keauhou 2 Ballroom
10:30 a.m.–12:30 p.m.
WB • Nonlinear Processes in Guided-Wave Geometries
Herbert G. Winful; Univ. of Michigan, USA, Presider

WB1 • 10:30 a.m. Invited

Slow, Fast, and Backwards Light Propagation in Erbium-Doped Optical Fibers, *Robert W. Boyd, George M. Gehring, Giovanni Piredda, Aaron Schweinsberg, Zhimin Shi, Heedeuk Shin, Joseph Vornehm, Petros Zerom; Univ. of Rochester, USA.* Erbium-doped optical fiber can serve as either a saturable absorber or (when pumped) as a saturable amplifier, leading to slow or fast light propagation respectively. Exotic propagation effects are observed in this system.

WB2 • 11:00 a.m.

Suppression of Stimulated Brillouin Scattering in High Power, Narrow Linewidth Fiber Amplifiers, *Stuart Gray, Donnell Walton, Ji Wang, Anping Liu, Ming-Jun Li, Xin Chen, A. Boh Ruffin, Jeffrey DeMeritt, Luis Zenteno; Corning Inc., USA.* Stimulated Brillouin scattering in optical fibers is suppressed by spatially separating the optical and acoustic modes. Using this technique, we demonstrate 500 Watts of output power from a single mode, narrow linewidth fiber amplifier.

WB3 • 11:15 a.m.

Supercontinuum Generation and Soliton Timing Jitter in SF6 Photonic Crystal Fibers, *Anatoly Efimov[1], Antoinette J. Taylor[1], Fiorenzo G. Omenetto[2], Jonathan C. Knight[3]; [1]Los Alamos Natl. Lab, USA, [2]Tufts Univ., USA, [3]Univ. of Bath, UK.* Using XFROG and FROG we observe the details of supercontinuum formation and soliton dynamics in highly-nonlinear SF6 photonic crystal fibers. At high input powers in the anomalous dispersion region the solitons display substantial temporal jitter.

WB4 • 11:30 a.m.

Saturation Absorption Spectroscopy in an Integrated Rubidium Vapor Cell, *Holger Schmidt[1], Wenge Yang[1], Bin Wu[1], Don B. Conkey[2], John Hulbert[2], Aaron R. Hawkins[2]; [1]Univ. of California at Santa Cruz, USA, [2]Brigham Young Univ., USA.* We demonstrate integrated rubidium vapor cells using hollow-core ARROW waveguides on a silicon chip. Optical mode areas of 8.8 square microns are promising for nonlinear optical applications. Saturation spectroscopy on the Rb-D2 line is demonstrated.

WB5 • 11:45 a.m.

Interactions of Chirped and Chirp-Free Similaritons in Optical Fiber Amplifiers, *Sergey Ponomarenko[1], Govind P. Agrawal[2]; [1]Dalhousie Univ., Canada, [2]Univ. of Rochester, USA.* We obtain exact self-similar solutions to a generalized nonlinear Schrödinger equation, (GNLSE). We show that despite the exact integrability of the GNLSE, single-similariton interactions can lead to the formation of the two-similariton bound states.

WB6 • 12:00 p.m.
Self Focusing of Surface Plasmon Polariton and Nonlinear Response of Plasmonic Waveguiding by Ponderomotive Forces, *Pavel Ginzburg, Alex Hayat, Eyal Feigenbaum, Nikolai Berkovitch, Meir Orenstein; Dept. of Electrical Engineering, Technion, Israel.* Extraordinary self focusing of single-interface plasmon polariton is proposed. Initial study of the nonlinear spectral shaping in plasmonic waveguide configurations is studied experimentally.

WB7 • 12:15 p.m.
Spatial Solitons in Azobenzene Liquid Crystals, *Svetlana Serak, Nelson Tabiryan; BEAM Engineering for Advanced Measurements Co., USA.* Reversible photoisomerization of azobenzene liquid crystal molecules allows formation of solitons at microwatt power levels of a He-Ne laser beam. Steering, deflection, merging and all-optical switching of spatial solitons were observed.

Keauhou Ballroom Foyer
10:00 a.m.–10:30 a.m.
Coffee Break

Keauhou Ballroom Foyer
10:00 a.m.–12:30 p.m.
Exhibits

WC • Nonlinear Optical Materials

Keauhou 3 Ballroom
10:30 a.m.–12:45 p.m.
WC • Nonlinear Optical Materials
Martti Kauranen; Tampere Univ. of Technology, Finland, Presider

WC1 • 10:30 a.m.
Using Numerical Optimization Techniques and Conjugation Modulation to Design the Ultimate Nonlinear-Optical Molecule, *Mark G. Kuzyk[1], Juefei Zhou[1], Urszula B. Szafruga[1], David S. Watkins[1], Javier Pérez-Moreno[1,2], Yuxia Zhao[3]; [1]Washington State Univ., USA, [2]Univ. of Leuven, Belgium, [3]Technical Inst. of Physics and Chemistry, Chinese Acad. of Sciences, China.* Guided by numerical calculations and sum rules, we made and characterized molecules with varying degrees of modulated conjugation between donor and acceptor ends. Hyper-Rayleigh scattering measurements of the best molecule show a record intrinsic hyperpolarizability.

WC2 • 10:45 a.m.
Variability of Orientation-Patterned GaAs Optical Parametric Oscillator Performance, *Scott A. Shell[1], Rita D. Peterson[2], Scott D. Lewis[2]; [1]Air Force Inst. of Technology, USA, [2]AFRL, USA.* OPO performance in 2-micron-pumped OPGaAs samples grown on different templates was found to be comparable, but exhibited significant variation within and between samples. Measured signal and idler wavelength values agreed closely with theory.

WC3 • 11:00 a.m. Invited
Novel Nonlinear Borate and Fluoroborate for Frequency Conversion: From Crystal Growth to Nonlinear Optical Properties, *Pascal Loiseau, Gerard Aka; Ecole Natl. Superieure de Chimie de Paris, France.* Nonlinear $Ca_4REO(BO_3)_3$ (RE = Gd, Y, Sc, Lu, Nd) offers opportunities of large dimension crystals and efficient non linear properties for practical applications with low or high power sources, from UV to visible range.

WC4 • 11:30 a.m.
Single-Event Effects Induced by Through-Wafer Sub-Bandgap Two-Photon Absorption, *Dale McMorrow[1], William T. Lotshaw[1], Joseph S. Melinger[1], Phillip Jenkins[1], Paul Eaton[2], Joseph Benedetto[2], Matt Gadlage[3], John D. Davis[4], Reed K. Lawrence[4], Daniel Loveless[5], Lloyd Massengill[5]; [1]NRL, USA, [2]Micro-RDC, USA, [3]NAVSEA Crane, USA, [4]BAE Systems, USA, [5]Vanderbilt Univ., USA.* Carrier generation based on nonlinear absorption in semiconductors has become an important tool for the investigation of single-event effects in modern microelectronic devices. TPA-induced single-event upset mapping and backside, through-wafer charge injection are described.

WC5 • 11:45 a.m.
Energy Band-Gap Dependence of Three-Photon Absorption in Semiconductors, *Peter D. Olszak[1], Scott Webster[1], Lazaro A. Padilha[1], Claudiu M. Cirloganu[1], Milton Woodall[2], David J. Hagan[1], Eric W. Van Stryland[1]; [1]College of Optics and Photonics, CREOL and FPCE, Univ. of Central Florida, USA, [2]DRS Infrared Technologies, LP, USA.* The bandgap and wavelength scaling of three-photon absorption (3PA) is studied in several semiconductors by the Z-scan technique. The 3PA coefficient is found to vary as Eg^{-7} as predicted by theory.

WC6 • 12:00 p.m.
Ultrafast Observation of the Coexistence of Antiferromagnetism and Superconductivity in a High-T_c Superconductor, *Elbert Chia[1], Jian-Xin Zhu[1], Diyar Talbayev[1], In-Sun Jo[2], Kyu-Hwan Oh[2], Sung-Ik Lee[2], Richard D. Averitt[3], Antoinette J. Taylor[1]; [1]Los Alamos Natl. Lab, USA, [2]Pohang Univ. of Science and Technology, Republic of Korea, [3]Boston Univ., USA.* Ultrafast quasiparticle dynamics of the high-*Tc* superconductor $Tl_2Ba_2Ca_2Cu_3O_y$ were probed using the all-optical pump-probe technique. Our results are consistent with the coexistence of antiferromagnetism and superconductivity at low temperatures.

WC7 • 12:15 p.m.
k-Space Spectroscopy: Investigation of a Size Dependent Phase Transition Behavior of Ferroelectric Domains, *Uwe Voelker, Urs Heine, Klaus Betzler; Dept. of Physics, Univ. of Osnabrueck, Germany.* We report on a technique for the measuring of ferroelectric domain structuring (k-space spectroscopy). Momentum conservation for optical second harmonic generation is achieved by the Fourier representation of the domain structuring (random quasiphase matching).

WC8 • 12:30 p.m.
Modeling of Thermal Lensing in Nonlinear Optical Crystals, *William A. Wood, David W. Lambert, Dmitri V. Kuksenkov; Corning Inc., USA.* An iterative approach to modeling thermal lensing in $\chi 2$ frequency conversion processes is described. Careful consideration is given to ensuring consistency of approximations. We find piezo-optic effects can partially compensate the impact of thermal dispersion.

Keauhou Ballroom Foyer
2:00 p.m.–5:30 p.m.
Exhibits

WD • Photonic Crystal Microcavities

Keauhou 2 Ballroom
2:00 p.m.–3:30 p.m.
WD • Photonic Crystal Microcavities
Kerry Vahala; Caltech, USA, Presider

WD1 • 2:00 p.m. Invited

Dynamic Control of Light by High-*Q* Photonic Crystal Nanocavities, *Masaya Notomi; NTT Basic Res. Labs, Japan.* Recent progress in ultrahigh-*Q* and ultrasmall cavities based on photonic-crystal slabs have impacts on various phenomena. Recent investigations of all-optical bistable switching, novel adiabatic wavelength conversion and opto-mechanical energy conversion employing these nanocavities.

WD2 • 2:30 p.m. Invited

Photonic-Crystal Nanocavities and Their Applications, *Susumu Noda; Kyoto Univ., Japan.* No abstract available.

WD3 • 3:00 p.m. Invited

Nonlinear Optical Processes in Photonic Crystal Microcavities, *Jelena Vuckovic; Stanford Univ., USA.* Photonic crystal cavities with ultra-small mode volumes and high *Q*-factors demonstrate 20GHz optical switching with 60fJ pulses, lasers operating at W thresholds and modulation speeds approaching THz, and a single quantum-dot control of cavity spectrum.

WE • NLO Poster Session

Keauhou 1 Ballroom
3:30 p.m.–6:00 p.m.
WE • NLO Poster Session

WE1

Detection of High-Speed Optical Modulation Signal by Using Difference-Frequency-Generation in Periodically-Poled $LiTaO_3$, *Hiroshi Murata, Yasuyuki Okamura; Osaka Univ., Japan.* The detection of a 15GHz optical modulation signal using DFG was demonstrated experimentally in periodically-poled $LiTaO_3$ with a microwave resonator structure. It leads to high-speed optical clock/vector-modulation signal detection devices for optical fiber communication systems.

WE2

Reduction of Nonlinear Phase Noise on PSK Signals by a Phase-Preserving Amplitude Limiter, *Masayuki Matsumoto; Osaka Univ., Japan.* Analysis is presented on the reduction of nonlinear phase noise in phase-shift-keying signal transmission by use of phase-preserving amplitude limiter based on saturation of FWM in fiber. Influence of imperfections of the limiter is discussed.

WE3

Optical Regeneration Using Nonlinear Interaction in Slow-Wave Microring Resonator Chains, *Pedro Chamorro-Posada[1], Francisco J. Fraile-Peláez[2]; [1]Univ. de Valladolid, Spain, [2]Univ. de Vigo, Spain.* We propose the use of slow-wave micro-ring resonator chains with saturable loss as optically controllable group delays for the retiming of optical signal in communication links. The proposed scheme is analyzed using numerical simulation.

WE4

Optical Sum Frequency Microscopy for Analyzing Starch in a Water Plant, *Goro Mizutani[1,2], Yoshihiro Miyauchi[1,2], Haruyuki Sano[1,2]; [1]Japan Advanced Inst. of Science and Technology, Japan, [2]CREST, Japan Science and Technology Agency, Japan.* It is demonstrated that non-destructive chemical analysis of starch granules in a water plant can be performed by using optical sum frequency microscopy with visible and infrared excitation.

WE5

Self-Organized Copper Nanowires Studied by Second Harmonic Spectroscopy, *Kitsakorn Locharoenrat[1,2], Haruyuki Sano[1], Goro Mizutani[1,2]; [1]Japan Advanced Inst. of Science and Technology (JAIST), Japan, [2]JAIST 21st COE Program, Japan.* We demonstrate that the local field near Cu nanowires enhanced by the plasmon excitation gives rise to second harmonic response when the excitation optical field is polarized perpendicular to the wire axes.

WE6

Nonlinear Optics in Quantum Structures with Long-Period Linear Grating Phasematching, *Alex Hayat, Eran Small, Yotam Elor, Meir Orenstein; Dept. of Electrical Engineering, Technion, Israel.* We developed a method for phasematching by long-period linear grating and employed it for highly nonlinear semiconductor QW structures in photonic waveguides both theoretically and experimentally where gratings were fabricated using focused ion beam.

WE7

Phase-Modulated Control of Hong-Ou-Mandel Two-Photon Interference, *Andrea T. Joseph, Roger Andrews; Univ. of the West Indies, Trinidad and Tobago.* We describe temporal control of two-photon interference of narrowband noncollinear type-I down-converted photons using symmetric spectral phase modulation. We find that the interference-fringe intensities can be controlled using the modulation depth and frequency.

WE8

High Two Photon Absorption of CdS Nanocrystal in Reverse Micelle Embedded in a Thin Film, *Yongwang Gao, Alberto Tonizzo, Ardie Walser, Mary Potasek, Roger Dorsinville; City College and Graduate Ctr. of The City Univ. of New York, USA.* Hybrid nanocomposites of surfactant-capped CdS nanoparticles embedded in polystyrene (PS) matrixes have been prepared and characterized. High two photon absorption coefficient values (> 250 cm/GW) were measured with pulses of 25ps duration at 532nm.

WE9

Nonlinear Optics in QWs with Tunable Local Phasematching, *Pavel Ginzburg, Alex Hayat, Meir Orenstein; Dept. of Electrical Engineering, Technion, Israel.* We propose a local phasematching approach based on QWs which provide both nonlinearity enhancement and the required dispersion relations. Optical susceptibilities of the structure can be tuned by applied voltage to match the design requirements.

WE10

Measurement of Nonlinear Absorption and Refraction in Doped Si Below the Band Edge, *William T. Lotwhaw, Dale McMorrow, Joseph S. Melinger; NRL, USA.* Quantitative laser single-event effects testing of microelectronics at sub-bandgap wavelengths requires detailed knowledge of material nonlinear-optical properties. Nonlinear absorption and refraction in Si were measured by femtosecond z-scans at several wavelengths near the band edge.

WE11

Excited State Absorption Cross-Sections of a Novel Terpyridyl Platinum (II) Complex, *Timothy M. Pritchett[1], Michael J. Ferry[1], Andrew G. Mott[1], William Shensky[2], Fengqi Guo[3], Bingguang Zhang[3], Wenfang Sun[3]; [1]U.S. ARL, USA, [2]General Technical Services, LLC, USA, [3]North Dakota State Univ., USA.* The absorption cross-sections of the singlet and triplet excited states of a novel terpyridyl platinum (II) complex have been measured using *Z*-scans at picosecond and nanosecond pulse widths and a variety of pulse energies.

WE12

Achieving Slow Light in Noninstantaneous Self-Defocusing Medium by Induced Modulation Instability, *Wen-Han Chu, Ming-Feng Shih; Natl. Taiwan Univ., Taiwan.* We demonstrate the slow speed of a sinusoidally modulated light train in a noninstantaneous self-defocusing medium by induced modulation instability.

WE13

Elliptically Modulated Self-Trapped Beams In Highly Nonlocal Nonlinear Media, *Servando Lopez-Aguayo, Julio Cesar Gutierrez-Vega; Photonics and Mathematical Optics Group, Tecnológico de Monterrey, Mexico.* We introduce a novel class of elliptically modulated spatial optical solitons in highly nonlocal nonlinear media. We also obtain elliptically self-trapped intensity rotating beams. The results obtained can be extended to general nonlocal nonlinear media.

WE14

Steady-State Solutions for Nonlinear Waveguide Equation up to Self-Focusing Limit, *Liang Dong; IMRA America Inc., USA.* Equation is obtained for solutions of nonlinear waveguide equation using Gaussian mode approximation. Critical power for nonlinear self-focusing is found independent of waveguide parameters, while steady-state solutions below self-focusing limit depend on V parameter.

WE15

Solitons in Bragg Gratings with Saturable Nonlinearity, *Ilya M. Merhasin[1,2], Boris A. Malomed[3], Krishnamoorthy Senthilnathan[1], K. Nakkeeran[4], P. K. A. Wai[1], K. W. Chow[5]; [1]Hong Kong Polytechnic Univ., Hong Kong, [2]Dept. of Electrical and Electronic Engineering, The College of Judea and Samaria, Israel, [3]Tel Aviv Univ., Israel, [4]Univ. of Aberdeen, UK, [5]Univ. of Hong Kong, Hong Kong.* Coupled-mode equations for two waves coupled by the Bragg reflection in the presence of saturable nonlinearity are introduced. Stable solitons and their bound states fill a part of the bandgap, their collisions being quasi-elastic.

WE16

Interplay of Photorefractively Recorded Parasitic Gratings and Photo-Induced Ferroelectric Structures, *Andreas Selinger, Uwe Voelker, Volker Dieckmann, Mirco Imlau; Univ. of Osnabrueck, Germany.* The interplay of photorefractively recorded parasitic gratings and photo-induced ferroelectric structures is uncovered in Fe-doped $LiNbO_3$. The phenomenon results in polarization-anisotropic light scattering appearing as segments of two cones upon exposure to a single pump-beam.

WE17

Surface Lattice Solitons: Analytical Solutions of a Kronig-Penney Model, *Yannis Kominis, Aristides Papadopoulos, Ilias Tsopelas, Sotiris Droulias, Nikos Efremidis, George Papazisimos, Kyriakos Hizanidis; Natl. Technical Univ. of Athens, Greece.* A novel phase-space method is employed for the construction of analytical stationary solitary waves located and robustly propagating at the interface between a periodic nonlinear Kronig-Penney lattice and a linear or nonlinear homogeneous medium.

WE18

Helmholtz-Gauss Self-Trapped Modes in Highly Nonlocal Nonlinear Media, *Servando Lopez-Aguayo, Julio Cesar Gutierrez-Vega; Photonics and Mathematical Optics Group, Tecnológico de Monterrey, Mexico.* We obtain an analytical expression to describe self-trapped beams in highly nonlocal nonlinear media; we show their direct relation with the so-called nondiffracting beams. The results obtained can be extended to general nonlocal nonlinear media.

WE19

Solitary Wave Propagation and Stabilization in Negative Index Materials, *Partha P. Banerjee, Georges Nehmetallah; Univ. of Dayton, USA.* Spatio-temporal multi-dimensional propagation in negative index materials is analyzed starting from a simple dispersion relation and a cubic nonlinearity. Using fast Fourier-Bessel numerical methods, we show that nonlinearity and/or dispersion management stabilizes solitary wave solutions.

WE20

All-Optical De-Multiplexing by Cross-Phase Modulation in Pattern-Independent Semiconductor Optical Amplifiers, *Claudio Crognale[1], Vittorio Ricchiuti[1], Stefano Caputo[2], Sante Saracino[3]; [1]TechnoLabs S.p.A., Italy, [2]SMD Elettronica, Italy, [3]Siemens S.p.A., Italy.* The features of an ultra-fast all-optical SOA-based interferometric de-multiplexer are investigated. It is shown how a proper management of the SOAs nonlinearities can improve the de-multiplexer performances, preserving the extracted channel integrity from the pattern-dependence.

WE21

Nonlinear Self-Carved Circular Cavities in Gap Subspace, *Eyal Feigenbaum, Meir Orenstein; Technion, Israel.* Optical spatial solitons, exhibiting closed loop orbital propagation within a gap between metal (or dielectric) layers, are presented. Obeying a novel modified NLSE these hybrid plasmon-solitons, are carving their own circular cavity.

WE22

Overcoming Traditional Manufacturing Limitations in High-*Q* Micro-Ring Resonators Using Nonlinear Effects in Silicon, *Michael D. Schmidt, Qianfan Xu, Michal Lipson, Hod Lipson; Cornell Univ., USA.* High sensitivity to fabrication errors is a main challenge in using high-*Q* resonators. Here we show that by carefully choosing the optical tuning using an evolutionary algorithm, a drastically distorted transmission function can be restored.

WE23

k-Spectra of the Uniaxial Relaxor Ferroelectric $Sr_xBa_{1-x}Nb_2O_6$ (SBN), *Uwe Voelker, Urs Heine, Rainer Pankrath, Klaus Betzler; Dept. of Physics, Univ. of Osnabrueck, Germany.* We present k-spectra of the ferroelectric SBN showing that domains react size-dependent at the phase transition and on external electric fields. Thus, all models assuming domains in SBN to behave uniquely have to be reconsidered.

WE24

Temperature Dependence of the Coercive Field of Vapour Transport Equilibrated Nearly Stoichiometric Lithium Tantalate, *Volker Wesemann[1], Alexander Quosig[2], Daniel Rytz[1], Johannes A. L'huillier[2]; [1]FEE GmbH, Germany, [2]Technische Univ. Kaiserslautern, Germany.* We investigated the dependence of the coercive field on the temperature for VTE prepared lithium tantalate. Between 13°C and 80°C, the coercive field of lithium tantalate with 49.96mol% Li_2O content decreased from 256V/mm to 198V/mm.

WE25

Accurate Determination of Nonlinear Optical Coefficients of Hexagonal Silicon Carbide of Polytype 6H, *Makoto Abe[1], Koichi Maruyama[2], Hiroaki Sato[2], Hiroaki Tanaka[2], Jun Suda[3], Ichiro Shoji[2], Takashi Kondo[1]; [1]Dept. of Materials Engineering, The Univ. of Tokyo, Japan, [2]Dept. of Electrical, Electronic, and Communication Engineering, Chuo Univ., Japan, [3]Dept. of Electronic Science and Engineering, Kyoto Univ., Japan.* Nonlinear optical cefficioents of 6H-SiC have been measured with much improved accuracy using high quality single crystalline plane-parallel plates by the Maker-fringe technique combined with theoretical analysis taking into account of the multiple-reflection effect.

WE26

Nonlinear Interactions of Space-Charge Waves in Semi-Insulating Materials, *Michaela Lemmer[1], Manfred Wöhlecke[1], Mirco Imlau[1], Mikhail P. Petrov[2]; [1]Univ. of Osnabrueck, Germany, [2]Ioffe Physico Technical Inst., Russian Acad. of Sciences, Russian Federation.* The method of resonant space-charge wave excitation is applied to classical high resistive semiconductors. Theoretical predictions for space-charge wave effects are experimentally verified enabling the determination of important material parameters.

WE27

Second Harmonic Generation by $BaTiO_3$ Microparticles in Porous Materials, *Susanne Lisinski[1], Dominik Schaniel[2], Theo Woike[2], Lorenz Ratke[1], Mirco Imlau[3]; [1]DLR, Inst. für Materialphysik im Weltraum, Germany, [2]Univ. zu Köln, Germany, [3]Univ. Osnabrück, Germany.* We present novel designed hybrid xerogels, where microparticles of nonlinear optical materials, especially $BaTiO_3$, are embedded in a porous silica matrix. The synthesis and second harmonic generation properties of these hybrid materials are described.

WE28

Frequency-Doubling of High-Power CW Laser Light in PPKTP, PPMgSLT, and PPMgLN, *F. J. Kontur, I. Dajani, Yalin Lu, R. J. Knize; Laser and Optics Res. Ctr., USA.* Frequency-doubing in PPKTP, PPMgSLT, and PPMgLN is studied for CW fundamental powers up to 10 W. Effects such as pump depletion and thermal dephasing are found to reduce conversion efficiency by 50% or more.

WE29

Investigation of Nd^{3+}: $(La_{1-x}Ba_x)F_{3-x}$ as New Vacuum Ultraviolet Scintillator and Potential Laser Material, *Marilou M. Cadatal[1,2], Young-Seok Seo[3], Toshihiro Tatsumi[3], Minh Pham[1,2], Carlito Ponseca[1,2], Shingo Ono[4], Elmer Estacio[3], Yusuke Furukawa[3], Hidetoshi Murakami[3], Yasushi Fujimoto[3], Nobuhiko Sarukura[3,1], Masahiro Nakatsuka[3], Kentaro Fukuda[5], Rayko Simura[5], Toshihisa Suyama[6], Akira Yoshikawa[5], Tsuguo Fukuda[5]; [1]Laser Res. Ctr., Inst. for Molecular Science, Japan, [2]Graduate Univ. for Advanced Studies, Japan, [3]Inst. of Laser Engineering, Osaka Univ., Japan, [4]Opto-Electronics Lab, Nagoya Inst. of Technology, Japan, [5]Inst. of Multidisciplinary Res. for Advanced Materials, Tohoku Univ., Japan, [6]Tokuyama Corp., Japan.* Nd^{3+}: $(La_{1-x}Ba_x)F_{3-x}$ as new scintillator and laser material is explored using efficient micro-PD method. Fluorescence peak located at 175 nm is better compared to Nd^{3+}:LaF_3 due to broader fluorescence and shorter VUV transmission edge.

WE30

Accurate Measurements of Second-Order Nonlinear-Optical Coefficients of Near-Stoichiometric $LiNbO_3$ at 1.31 and 1.06μm, *Ichiro Shoji[1], Tatsuro Ue[1], Kei Hayase[1], Akinori Arai[1], Makoto Takeda[1], Satoshi Nakajima[1], Akinori Neduka[2], Ryoichi Ito[2], Yasunori Furukawa[3]; [1]Chuo Univ., Japan, [2]Meiji Univ., Japan, [3]Oxide Corp., Japan.* Second-order nonlinear-optical coefficients of undoped and MgO-doped near-stoichiometric $LiNbO_3$ are measured at the fundamental wavelengths of 1.31 and 1.06μm. The values are found nearly the same with those of congruent $LiNbO_3$ within the experimental accuracy.

WE31

Electromagnetic Contribution to Surface Enhanced Raman Scattering of Rhodamine 6G Molecules on Rice-Shaped Au Nanocrystals, *JaeTae Seo[1], Liting Huang[1], Jinhwa Heo[2,3], Lisa Brodsky[1], WanJoong Kim[2], Qiguang Yang[1], Bagher Tabibi[1], Sungsoo Jung[2], Wansoo Yun[2], Sangwoo Han[3], Min Namkung[4]; [1]Hampton Univ., USA, [2]Korea Res. Inst. of Standards and Science, Republic of Korea, [3]Gyeongsang Natl. Univ., Republic of Korea, [4]NASA Goddard Space Flight Ctr., USA.* The factor of electromagnetic contribution to SERS of Rh_6G on rice-shaped Au nanocrystals was estimated to be around six-order higher than Raman scattering of Rh_6G.

WE32

Surface Enhanced Raman Scattering (SERS) with Arrays of Nanoholes on Aluminum Oxide, *Haim Grebel, Chichang Zhang, Kakhkhor Abdijalilov; NJIT, USA.* We examine the usefulness of aluminum and nanoporous alumina platforms for SERS applications through examples of carbon nanotubes, C60 and soft biospecies.

WE33

Nonlinear Couplings between Higher Order Modes in 2nd Order Nonlinear Interactions, *Preben Buchhave; Technical Univ. of Denmark, Denmark.* We present a realistic method for dynamic simulation of interactions in a nonlinear crystal. The deformation of the wave fronts due to the nonlinear interaction is expressed by expansion in higher order Gauss-Hermite modes.

WE34

Design of Coupled-Defect Thin-Film Stacks for All-Optical Spatial Beam Switching, *Felix Gloeckler, Uli Lemmer, Martina Gerken; Lichttechnisches Inst., Germany.* Periodic Bragg stacks with one and two defect cavities are numerically investigated for all-optical photonic crystal superprism switching. Maximum achievable shifts and necessary switching powers are evaluated depending on the position of the nonlinear material.

WE35
Study on the Field-Poling Dynamics in Mg-Doped $LiNbO_3$ and $LiTaO_3$, *Hideki Ishizuki, Takunori Taira; Laser Res. Ctr., Inst. for Molecular Science, Japan.* Response characteristics of Mg-doped congruent $LiNbO_3$, and $LiTaO_3$ at the field-poling process was evaluated using ramping-electric field with several ramping rates, and compared with undoped crystals. Field-poling dynamics was different between Mg-doped and undoped crystals.

Hawaii Lawn & Crystal Blue Point
6:00 p.m. – 8:00 p.m.
Conference Luau

•Thursday, August 2, 2007•

Keauhou Ballroom Foyer
7:30 a.m. – 12:30 p.m.
Registration Open

ThA • Plenary III

Keauhou 3 Ballroom
8:00 a.m.–10:00 a.m.
ThA • Plenary III
George Stegeman; Univ. of Central Florida, USA, Presider

ThA1 • 8:00 a.m. Plenary
Clocks, Combs and Optical Arbitrary-Waveform Generators, *Erich Ippen; MIT, USA.* No abstract available.

ThA2 • 9:00 a.m. Invited
Advances in Femtosecond Fiber Lasers, *Frank Wise; Cornell Univ., USA.* A new pulse-shaping process enables the construction of the first femtosecond lasers that do not require intracavity dispersion control. These lasers to generate pulses with energies 10-20 nJ, comparable to the performance of solid-state lasers.

ThA3 • 9:30 a.m.
Amplitude Noise of Femtosecond Fiber Lasers in Different Modelocking Regimes, *Levent Budunoglu, Fatih Ömer Ilday; Bilkent Univ., Turkey.* Amplitude noise of femtosecond fiber laser oscillators are characterized in soliton, similariton, stretched-pulse and all-normal GVD regimes of mode-locking. Integrated relative intensity noise as low as 0.023% (1 Hz - 100 kHz) is reported.

ThA4 • 9:45 a.m.
Single-Cycle Optical Pulses with Constant Carrier-Envelope Phase, *Wei-Jan Chen[1], Zhi-Ming Hsieh[1], Shu Wei Huang[2], Hao-Yu Su[1], A. H. Kung[1,3]; [1]Inst. of Atomic and Molecular Sciences, Academia Sinica, Taiwan, [2]MIT, USA, [3]Natl. Chiao-Tung Univ., Taiwan.* 1.5 femtosecond long single-cycle optical pulses that have a constant envelope phase are constructed from commensurate vibrational Raman sidebands produced by molecular modulation in room temperature H_2.

Keauhou Ballroom Foyer
10:00 a.m.–10:30 a.m.
Coffee Break

Keauhou Ballroom Foyer
10:00 a.m.–12:30 p.m.
Exhibits

ThB • Attosecond and X-Ray Generation

Keauhou 3 Ballroom
10:30 a.m.–12:30 p.m.
ThB • Attosecond and X-Ray Generation
Stephen E. Harris; Stanford Univ., USA, Presider

ThB1 • 10:30 a.m. Invited
Attosecond X-Ray Photonics: All-Optical Quasi-Phase Matching for High Harmonic Generation, *Oren Cohen, Xiaoshi Zhang, Amy Lytle, Henry Kapteyn, Margaret Murnane; JILA, Univ. of Colorado, USA.* We use counterpropagating pulse trains to selectively enhance high-order harmonic generation from 70eV to 145eV using all-optical quasi phase matching. Enhancement factors up to x400 are obtained.

ThB2 • 11:00 a.m.
A Proposed Tabletop Optical MEMs-Based Atto-Second Pulse Coherent Soft X-Ray Source, *Tomas Plettner, Robert L. Byer; E.L. Ginzton Labs, USA.* We propose a MEMs based photonic device micro-undulator powered by a laser-driven particle accelerator as an effective means for generating coherent SASE-FEL X-ray pulses in the attosecond timescale.

ThB3 • 11:15 a.m. Invited
Xe Plasma Generated by a Cavity Enhanced Yb-Similariton Laser Based Fiber Frequency Comb, *Ingmar Hartl[1], A. Marcinkevicius[1], M. E. Fermann[1], T. R. Schibli[2], D. D. Hudson[2], D. C. Yost[2], J. Ye[2]; [1]IMRA America, Inc., USA, [2]NIST and Univ. of Colorado, USA.* An Yb-fiber-frequency-comb-laser producing 75fs-pulses at 136MHz-repetition-rate and >10W-average-power is locked to a high-finesse cavity. A record intra-cavity average-power of up to 1.3kW and a peak-intensity of up to $8*10^{13}W/cm^2$ were reached, allowing ionization of Xe.

ThB4 • 11:45 a.m.
Density-Grating-Based Plasma Nonlinear Optics, *Jyhpyng Wang[1,2,3], Chih-Hao Pai[1,2], Szu-yuan Chen[1], Jiunn-Yuan Lin[4], Ming-Wei Lin[1], Kan-Hua Lee[1], Li-Chuang Ha[1]; [1]Inst. of Atomic and Molecular Sciences, Taiwan, [2]Natl. Taiwan Univ., Taiwan, [3]Natl. Central Univ., Taiwan, [4]Dept. of Physics, Natl. Chung Cheng Univ., Taiwan.* Nonlinear optics based on plasma density gratings is studied experimentally. Enhancement of relativistic third-harmonic generation by quasi-phase matching in periodic plasma waveguides is achieved, and degenerate four-wave mixing mediated by ponderomotive-force-driven plasma gratings is demonstrated.

ThB5 • 12:00 p.m. Invited
Compact 0.56 Petawatt Laser System Based on OPCPA, *Efim A. Khazanov, V. V. Lozhkarev, G. I. Friedman, V. N. Ginzberg, E. V. Katin, A. V. Kirsanov, G. A. Luchinin, A. N. Mal'shakov, M. A. Matryanov, O/ V. Palashov, A. K. Poteomkin, A. M. Sergeev, A. A. Shaykin, I. V. Yakovlev; Inst. of Applied Physics, Russian Federation.* 560TW power has been achieved experimentally using a Cr:forsterite master oscillator at 1250nm, a stretcher, three KD*P optical parametrical amplifiers providing 38J in chirped pulse at 910nm central wavelength, and a compressor providing 43fs pulse.

ThC • Postdeadline Session

Keauhou 3 Ballroom
7:30 p.m.–9:30 p.m.
ThC • Postdeadline Session
Franz X. Kaertner; MIT, USA.

•Friday, August 3, 2007•

Keauhou Ballroom Foyer
7:30 a.m. – 12:30 p.m.
Registration Open

FA • Novel Sources and Applications

Keauhou 3 Ballroom
8:00 a.m.–10:00 a.m.
FA • Novel Sources and Applications
Karl Koch; Corning, Inc., USA, Presider

FA1 • 8:00 a.m. **Invited**
High Intensity Fiber Lasers: From EUV Lithography to Hard X-Ray Generation, *Almantas Galvanauskas; Univ. of Michigan, USA.* No abstract available.

FA2 • 8:30 a.m.
A Master-Oscillator-Power-Amplifier 2-micron Laser Using Fiber Phase-Conjugate Mirror, *Jirong Yu[1], Yinxing Bai[2], Victor Leyva[3], V. Shkunov[3], David Rockwell[3], A. Betin[3], J. Wang[3], M. Petros[4], Paul Petzar[5], Bo Trieu[1], U. N. Singh[1]; [1]NASA Langley Res. Ctr., USA, [2]Science Systems and Applications Inc, USA, [3]Raytheon Co., USA, [4]Science and Technology Corp., USA, [5]Natl. Inst.ion of Aerospace, USA.* For the first time, a 2-micron master-oscillator-power-amplifier laser using a fiber based phase conjugation mirror has been demonstrated. The beam quality improvement and 56% of the PCM reflectivity have been achieved.

FA3 • 8:45 a.m.
High-Energy, Narrow-Bandwidth Periodically Poled MgO:LiNbO$_3$ Optical Parametric Oscillator with a Volume Bragg Grating, *Jiro Saikawa[1], Masaaki Fujii[1], Hideki Ishizuki[2], Takunori Taira[2]; [1]Tokyo Inst. of Technology, Japan, [2]Inst. for Molecular Science, Japan.* We demonstrated a high-energy, narrow-bandwidth, large aperture periodically poled MgO:LiNbO$_3$ optical parametric oscillator with a volume Bragg grating. Output energy of 50mJ with less than 1.5nm spectral bandwidth at 2.128μm was obtained.

FA4 • 9:00 a.m.
High Power Picosecond Laser Pulse Recirculation, *Miroslav Shverdin, Igor Jovanovic, David Gibson, Fred Hartemann, Scott G. Anderson, Curtis Brown, Shawn Betts, Jose Hernandez, Micah Johnson, Mike Messerly, Jason Pruet, Aaron Tremaine, Dennis McNabb, Craig Siders, Chris P. J. Barty; Lawrence Livermore Natl. Lab, USA.* We designed and constructed a nonlinear crystal-based short pulse recirculation cavity that traps the second harmonic of an incident high power laser. This scheme aims to increase the efficiency of Compton-scattering based light sources.

FA5 • 9:15 a.m.
Pumping a GaAs Optical Parametric Oscillator with Circularly Polarized and Depolarized Light, *Paulina S. Kuo[1], Konstantin L. Vodopyanov[1], Martin M. Fejer[1], Xiaojun Yu[1], Angie C. Lin[1], James S. Harris[1], David F. Bliss[2], Candace L. Lynch[2]; [1]Stanford Univ., USA, [2]AFRL, USA.* We demonstrate an optical parametric oscillator based on GaAs pumped with both a circularly polarized and a pseudo-depolarized pump. High symmetry in the nonlinear susceptibility tensor of GaAs enables pumping with "exotic" polarizations.

FA6 • 9:30 a.m. **Invited**
Nonlinear Optical Microscopy: From Imaging Molecular Dynamics to Blood Flow in Living Systems, *Jeffrey Squier[1], Dawn Schafer[1], Rob Applegate[1], Ramon Carriles[1], Wafa Amir[1], David Marr[1], Ralph Jimenez[2], Emily Gibson[1], Michiel Muller[3]; [1]Colorado School of Mines, USA, [2]Univ. of Colorado, USA, [3]Univ. of Amsterdam, Netherlands.* Nonlinear optical effects can be successfully exploited to generate a quantitative metric of molecular, organelle, cellular, and indeed organ-level dynamics as well as the very tools essential for these dynamic nonlinear optical studies.

Keauhou Ballroom Foyer
10:00 a.m.–10:30 a.m.
Coffee Break

Keauhou Ballroom Foyer
10:00 a.m.–12:30 p.m.
Exhibits

FB • Nonlinear Optics in Microresonators

Keauhou 3 Ballroom
10:30 a.m.–12:30 p.m.
FB • Nonlinear Optics in Microresonators
Susumu Noda; Kyoto Univ., Japan.

FB1 • 10:30 a.m. **Invited**
Nonlinear Opto-Mechanics Using Radiation Pressure in Micro-Cavities, *Kerry Vahala[1], Tal Carmon[1], Tobias Kippenberg[2], Mani Hosein Zadeh[1]; [1]Caltech, USA, [2]Max Planck Inst. fur Quantenoptik, Germany.* The union of optical microcavities and micro-mechanical resonators in certain devices has enabled a new, opto-mechanical coupling by radiation pressure. Recent work on mechanical oscillators and cooling is reviewed.

FB2 • 11:00 a.m.
Cooling of a Micro-Mechanical Oscillator Using Radiation-Pressure Induced Dynamical Backaction, *Albert Schliesser[1], Nima Nooshi[1], Pascal Del'Haye[1], Remi Rivière[1], Georg Anetsberger[1], Kerry Vahala[2], Tobias J. Kippenberg[1]; [1]Max-Planck-Inst. of Quantum Optics, Germany, [2]Caltech, USA.* We demonstrate how dynamical backaction of radiation pressure can be exploited for passive laser-cooling of high-frequency (>40 MHz) mechanical oscillation modes of ultra-high-finesse optical microcavities from room temperature to 8 K.

FB3 • 11:15 a.m. **Invited**
Optical Frequency Comb Generation from a Monolithic Micro-Resonator via the Kerr Nonlinearity, *Pascal Del'Haye, Albert Schliesser, Tobias Wilken, Ronald Holzwarth, Tobias Kippenberg; Max-Planck-Inst. for Quantum Optics, Germany.* It is shown that the cascaded optical sidebands generated via optical parametric oscillations in a monolithic microcavity are equidistant down to a resolution bandwidth limited level of 2 kHz.

FB4 • 11:45 a.m.
Visible Continuous Emission from a Silica Microphotonic Device by Third Harmonic Generation, *Tal Carmon, Kerry J. Vahala; Caltech, USA.* Continuous-wave, visible emission from a silica microresonator on silicon by third-harmonic generation is demonstrated. Emission is observed with pump powers <300μW. This result opens the possibility of silicon microphotonic devices spanning from UV to NIR.

FB5 • 12:00 p.m.

Mode Structure and Tunability of Adaptive, Hemispherical Microcavities, *Rebecca Pennington, Malgosia Kaczmarek, Giampaolo D'Alessandro, Jeremy Baumberg; Univ. of Southampton, UK.* Light propagation and spectra of micron-scale planar-hemispherical microcavities, both empty and filled with functional materials, were investigated. The cavities' are tunable and their modes have Laguerre-Gauss symmetry, but with unexpected spectral ordering of transverse modes.

FB6 • 12:15 p.m.

Optically-Pumped Semiconductor Disk Lasers for Second-Harmonic and Sum-Frequency Generation, *Antti Härkönen, Jussi Rautiainen, Janne Konttinen, Tomi Leinonen, Pietari Tuomisto, Lasse Orsila, Mircea Guina, Markus Pessa, Oleg G. Okhotnikov; Tampere Univ. of Technology, Finland.* We report on intracavity frequency-doubling and sum-frequency generation in optically-pumped semiconductor disk lasers. High power second-harmonic red emission from a GaInNAs-based disk laser and aquamarine sum-frequency emission from a dual-wavelength semiconductor disk laser were obtained.

NOTES

Key to Authors and Presiders

(BOLD denotes Presider or Presenting Author)

Nonlinear Optics: Materials, Fundamentals and Applications 2007 Topical Meeting and Tabletop Exhibit

UPDATE SHEET

Welcome to Kona and the Nonlinear Optics: Materials, Fundamentals and Applications Topical Meeting and Tabletop Exhibit. This promises to be a most informative and exciting meeting.

Program Events

Poster Session
Wednesday, August 1 * 3:30 p.m. – 6:00 p.m. * Keauhou Ballroom 1
Over 30 posters will be presented and light refreshments will be served. Poster presenters may set-up their posters starting at 1:00 p.m. Posters should be removed from the boards immediately following the conclusion of the session.

Conference Luau
Wednesday, August 1 * 6:00 p.m. – 10:00 p.m. * Hawaii Lawn & Crystal Blue Point
Join your colleagues for a traditional Hawaiian Luau. The cost of the luau is included in the price of registration for technical registrants. Guest tickets may be purchased at the registration desk by 12:00 p.m. on Monday, July 30.

Exhibits

Thank you to **Swamp Optics** for sponsoring the NLO 2007 Registration Bags.

We would like to thank **Taylor & Francis** for their NLO 2007 bag insert.

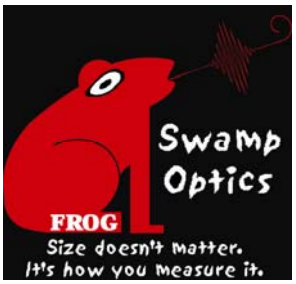

Taylor & Francis
Taylor & Francis Group

The Organizers of NLO 2007 gratefully acknowledge the support of:

Air Force Office of Scientific Research (AFOSR)

Defense Advanced Research Projects Agency (DARPA)

Program Changes

Author List Correction
WC1: **Using Numerical Optimization Techniques and Conjugation Modulation to Design the Ultimate Nonlinear-Optical Molecule,** *Mark G. Kuzyk[1], Juefei Zhou[1], Urszula B. Szafruga[1], David S. Watkins[1], Javier Pérez-Moreno[1,2], Koen Clays[1,2], Yuxia Zhao[3]; [1]Washington State Univ., USA, [2]Univ. of Leuven, Belgium, [3]Technical Inst. of Physics and Chemistry, Chinese Acad. of Sciences, China.*

Presider Updates
TuD. Nonlinear Optics in Si Nanostructures, Victor I. Klimov; *Los Alamos Natl. Lab, USA.*
WA. Metamaterials, Takunori Taira; *Laser Res. Ctr. for Molecular Science, Japan.*

Speaker Change
WC1: **Using Numerical Optimization Techniques and Conjugation Modulation to Design the Ultimate Nonlinear-Optical Molecule.** Presenter: Javier Pérez Moreno; *Washington State Univ., USA, and Univ. of Leuven, Belgium*.

Withdrawn Paper
MA3: **High-Efficiency Source of a Three-Photon W State and Its Full Characterization Using Quantum State Tomography**

Nonlinear Optics: Materials, Fundamentals and Applications
Postdeadline Papers

Keauhou 3 Ballroom
Thursday, August 2, 2007, 7:30 p.m.–8:45 p.m.
Franz X. Kaertner; MIT, USA, Presider

ThC1 ● 7:30 p.m.
World Record High Average Power Frequency Conversion with Large Aperture YCOB, *Kathleen Schaffers[1], A. J. Bayramian[1], J. A. Caird[1], R. Campbell[1], C. A. Ebbers[1], B. L. Freitas[1], R. Kent[1], D. Van Lue[1], Z. Liao[1], T. Ladran[1], S. Sutton[1], B. Chai[2], Y. Fei[2]; [1]LLNL, USA, [2]Crystal Photonics, Inc., USA.* This YCOB wavelength converter holds the current world record for an average-power high-pulse-energy laser at 227 W, 10 Hz, and 22.5 J per pulse. YCOB crystals have been scaled by a factor of 27.

ThC2 ● 7:45 p.m.
Tunable Nonlinear Beam Defocusing in Infiltrated Photonic Crystal Fibers, *Christian R. Rosberg[1], Francis H. Bennet[1], Dragomir N. Neshev[1], Per D. Rasmussen[2], Ole Bang[2], Wieslaw Z. Krolikowski[1], Anders Bjarklev[2], Yuri S. Kivshar[1]; [1]Australian Natl. Univ., Australia, [2]Technical Univ. of Denmark, Denmark.* We demonstrate a novel experimental platform for discrete nonlinear optics based on infiltrated photonic crystal fibers. We observe tunable discrete diffraction and nonlinear self-defocusing, and apply the effects to realize a compact all-optical power limiter.

ThC3 ● 8:00 p.m.
Multiwavelength Kilowatt-Peak-Power Light Pulse Source Utilizing a Picosecond Diode Laser for Nonlinear Bioimaging, *Hiroyuki Yokoyama[1], Keijiro Takashima[1], Masahito Mure[2], Hengchang Guo[1], Jun-ichi Shikata[3], Hiromasa Ito[3], Hiroshi Tsubokawa[4], Naoaki Saito[5]; [1]New Industry Creation Hatchery Ctr. (NICHe), Tohoku Univ., Japan, [2]New Technology Res. Labs, Sumitomo Osaka Cement Co., Ltd., Japan, [3]Res. Inst. of Electrical Communication (RIEC), Tohoku Univ., Japan, [4]Graduate School of Information Sciences, Tohoku Univ., Japan, [5]Biosignal Res. Ctr., Kobe Univ., Japan.* We generated octave-wide supercontinuum light with a diode-laser picosecond light source. The supercontinuum light was amplified to kilowatt peak-power levels by optical fiber amplifiers at three wavelength regions, and was successfully used for two-photon bioimaging.

ThC4 ● 8:15 p.m.
Inhomogeneous Tensorial Nonlinear Responses from an Array of Gold Nanoparticles, *Martti Kauranen[1], Hannu Husu[1], Brian K. Canfield[1], Juha Kontio[1], Jukka Viheriälä[1], Tuomo Rytkönen[1], Tapio Niemi[1], Eric Chandler[2], Alex Hrin[2], Jeff A. Squier[2]; [1]Tampere Univ. of Technology, Finland, [2]Colorado School of Mines, USA.* We use second- and third-harmonic-generation microscopy to address nonlinear responses of individual gold nanoparticles in an array. Widely-variable, polarization-dependent responses of individual particles indicate tensorial inhomogeneities in the sample.

ThC5 ● 8:30 p.m.
Chirped Biphotons Using Quasi Phase Matching, *S. Sensarn, S. E. Harris; Stanford Univ., USA.* We describe techniques for numerically simulating broadband, time-energy entangled biphoton generation by spontaneous parametric down conversion in quasi-phase-matched nonlinear crystals. Typical domain errors have negligible effect on the phase spectrum of the biphoton wavefunction.

World Record High Average Power Frequency Conversion with Large Aperture YCOB

K.I. Schaffers, A.J. Bayramian, J. A. Caird, R. Campbell, C.A. Ebbers, B.L. Freitas, R. Kent, D. Van Lue, Z. Liao, T. Ladran, and S. Sutton
Lawrence Livermore National Laboratory, 7000 East Ave., L-482, Livermore, CA 94550-9234 USA
Phone: (925)422-5084, FAX: (925)424-2495, email: schaffers1@llnl.gov

B. Chai and Y. Fei
Crystal Photonics, Inc 5525 Sanford Lane, Sanford, Fl 32773

Abstract: This YCOB wavelength converter holds the current world record for an average-power high-pulse-energy laser at 227 W, 10 Hz, and 22.5 J per pulse. YCOB crystals have been scaled by a factor of 27.

OCIS codes: (140.3580) Solid State Lasers; (190.4400) Nonlinear Optics

1. Introduction

The world record for average-power high-pulse-energy lasing (227 W) has been achieved with yttrium calcium oxyborate (YCOB) in the Mercury laser system. The previous world record for average-power frequency conversion was 165 W, 5 J/pulse reported by TRW. [1] The world's largest YCOB crystals have also been grown with a factor of 27 increase in size over past reports. Large aperture plates are harvested making it possible for a single *side-cooled* YCOB crystal to replace an assembly of four *face-cooled* potassium di-deuterium phosphate (DKDP) crystals and four sapphire cooling plates; one YCOB crystal replaces a complex assembly of eight optical elements. This system has been activated on the Mercury laser, a world-class diode-pumped solid state laser, based on a architecture scaleable to the multi-kilojoule energy levels with minimal beamline re-engineering [2]. The Mercury laser has already delivered over 50 J at an average power of 500 W (10 Hz, 15 ns) and is currently being upgraded for 100 J with an average power of 1000 W. Two unique, scaleable geometries for thermal and phase velocity management of YCOB crystals have been proven making it possible to achieve world record powers for frequency conversion from large apertures. By implementing a two-tier strategy for frequency conversion technology development, a low-risk baseline has been looked at as well as a moderate risk-high payoff solution. Our 'baseline' frequency conversion cooling technology employs a sapphire heat spreader concept to allow for more flexibility in crystal thickness and crystal geometries for the initial materials characterization. For the frequency conversion crystal we have tested two materials: DKDP whose growth to 40 cm apertures has already been demonstrated by the National Ignition Facility and YCOB, a crystal with very favorable thermo-optic characteristics compared to DKDP which can potentially be scaled to apertures of 20 cm. Our "moderate risk-high payoff solution cooling technology employs gas-cooling of YCOB slabs with high-speed helium in an adjustable architecture scaleable to multi-kilowatt apertures

2. Frequency Conversion Crystal

We choose our frequency conversion crystals based on the ability to perform second and third harmonic generation of 1047 nm with intrinsically low absorption. Recently, the nonlinear optical coefficients of two new oxyborates have been characterized [3,4]. YCOB has a significantly larger thermal acceptance (> 10 x) and fracture strength (10x) than DKDP. Most importantly, large aperture, world record, growth of YCOB has been recently demonstrated, producing 7.5 x 25 cm boules. The growth efforts are summarized in Figure 1(a), showing a large aperture boule with only a whisper of veiling near the bottom. From these boules we have fabricated full aperture (5.5 cm x 8.5 cm x 1.58 cm thick), defect free plates of YCOB for frequency conversion. Of the commercially available crystals (DKDP, LBO, KTP, BBO, GdCOB, YCOB) DKDP and YCOB have been chosen as the "baseline" and "advanced-concept" converter crystals, respectively. DKDP is a crystal with over 30 years of development effort with well-characterized material parameters such that the thermo-optical performance characteristics of DKDP can be reliably modeled. However, DKDP exhibits a relatively low fracture temperature (less than 10 C), requiring the use of multiple plates to minimize thermal gradients, making it desirable to implement new high performance materials such YCOB, described above.

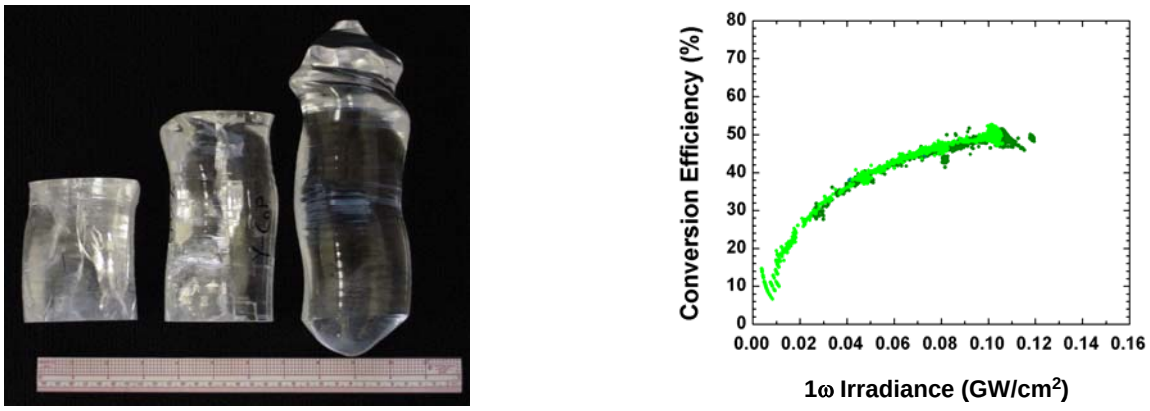

Figure 1(a). We fabricated 5.5 cm x 8.5 cm x 1.58 cm slabs from the boule on the left. (b) Conversion efficiency as a function of 1ω irradiance. We have obtained 227 W of 523 nm light at a conversion efficiency of 50%.

3. Cooling Technology

Currently the Yb:SFAP gain medium in the Mercury laser is cooled via a system involving gas cooling with high-speed helium where the slabs are separated by 1 mm helium flow channels. The total heat removed from each crystal is on the order of 35 W with a thermal loading of approximately 2 W/cm^2. This gas cooling technique has as a benefit the ability to scale to multi-kilowatt apertures. In contrast to the gain medium, nonlinear optical processes are elastic processes, with the thermal load arising strictly from the residual linear and nonlinear absorption in the crystal. Typical absorption coefficients for transparent crystals are on the order of 0.0025/cm, leading to an average power loading of 0.01 W/cm^2 on the Mercury 4.5 cm x 7.5 cm aperture beamline. These modest thermal loads lead to relatively small temperature gradients of 2-3 degrees C in the nonlinear optical crystal. Nevertheless, this gradient can lead to thermal dephasing (reduced conversion efficiency) or thermal fracture. Frequency conversion requires modifications of the gas cooling technology and gain medium design to introduce angular tuning capability and pointing adjustability. A typical pointing specification for critically phase-matched crystals is 250 μrad. The difficulty is that the typical vendor orientation capability is on order of 17,000 μrad (+/- 0.5 degrees) thereby requiring the need to individually rotate the crystal with respect to the beam propagation direction.

Although the gas-cooling technology has the advantage in that it is well developed, we require more flexibility in our experiments with the crystal thickness and conversion geometries. Therefore, another technology, recently utilized in an externally doubled high average power laser [5], has been commissioned, which relies on a highly thermally conductive and transparent substrate for cooling. We have chosen sapphire as the substrate since it is widely used as an optical window and has a relatively high thermal conductivity (0.3 W/cm/K) The frequency conversion cooler concept close couples the crystal to the sapphire plate (through a 30 micron air gap). Thermal modeling shows the sapphire face-cooled technology will scale to the required 20 cm aperture. The gas cooling and the heat spreader concepts are schematically shown in Figure 2.

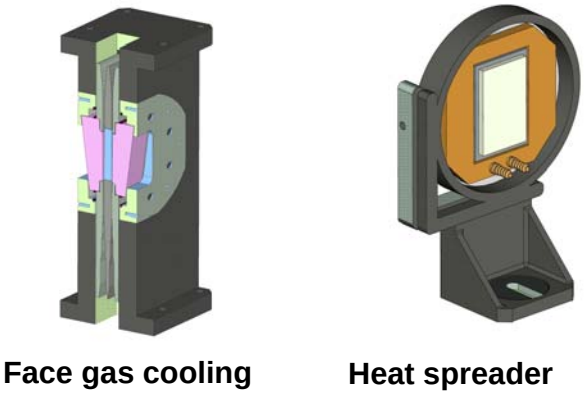

Figure 2. A heat-spreader cooling concept has been implemented (on the right) to manage the modest thermal loads present in the frequency conversion crystals.

4. Thermal performance

As previously discussed by Eimerl [6], even though the thermal loading on the nonlinear optical crystals is typically 100 times lower than the thermal loading on the gain medium, the need to maintain the phase velocities of the infrared and second harmonic light within the crystal to a small fraction of a wave is complicated by the relatively large value of the thermal change in the refractive indices. Even a modest temperature rise of a few degrees can result in significantly reduced conversion efficiencies. Thermal management by gas face-cooling has been shown to be scaleable to the 20-30 cm aperture for thermally loaded Yb:SFAP. Potential limitations include the gas temperature rise between the time the gas first picks up heat from the lasing medium or nonlinear optical crystal and as it exits past the crystal. The modest heat loading from the gas-cooled frequency converter does not impose any such aperture constraints. Due to the small amount of heat that needs to be removed from the frequency conversion crystals, this transverse thermal gradient (transverse to the beam propagation direction) is less than $1/10^{th}$ the longitudinal gradient (gradient across the thickness of the crystal) and has minor impact on the conversion efficiency. The side-cooled sapphire has limitations due to the need for heat transport across the sapphire optic before it is transferred to the cooling medium (water). Nevertheless, thermal modeling of the system indicates high conversion efficiency can be obtained, even with relatively large (20 cm) apertures. This cooling concept was tested utilizing a single 1.5 cm thick DKDP plate faced cooled by a 5 mm thick CaF_2 plate separated by a 30 micron air gap. We found that at an incident average power of 450 watts, the DKDP frequency converter did not display any sign of thermal dephasing during the 30 minute test run. Given the low drive, multiple (4) DKDP plates would be required for high conversion efficiency (greater than 50%). The single plate of DKDP had a conversion efficiency of approximately 12%, in agreement with modeling.

5. Average power frequency conversion

Utilizing a full aperture YCOB plate, the 550 W output of the Mercury laser (55 J, 10 Hz, 15 ns) was frequency converted, generating a record 227 W of average power at 523.5 nm. The beam was image relayed to an uncoated, side-cooled YCOB crystal with a thickness of 1.58 cm. The experimentally measured conversion efficiency, (Fig. 1b), matched the expected theoretical performance including the angular acceptance of the crystal. The frequency conversion assembly was operated with the incident average power of 550 W for a total of 30 minutes with no sign of optical damage (surface or internal). As the laser is brought to the higher output energy, we will utilize a YCOB doubler that is optimized for the higher fluence (a thinner crystal with a larger angular acceptance), with an expected conversion efficiency approaching 80%.

6. Summary

We have achieved a record average power performance from a side cooled YCOB crystal, producing an average power of 227 W at a conversion efficiency of 50%. In addition, YCOB crystals have been scaled by 27 times to achieve world record sizes. A two-tier strategy has been implemented to activate frequency conversion for the Mercury laser. We have chosen for our baseline cooling technology a heat spreader concept and have tested the thermal performance of DKDP with this technology. As a moderate risk – high payoff strategy we have modeled the thermal performance of a face and side cooled YCOB frequency conversion crystal.

This work was performed under the auspices of the U.S. Department of Energy by the University of California Lawrence Livermore National Laboratory under contract No. W-7405-Eng-48.

References

[1] R. J. St. Pierre, d. Mordaunt, H. Injeyan, J. G. Berg, R. C. Hilyard, M. E. Weber, M. G. Wickham, G. Harpole, "Diode array pumped kilowatt laser," SPIE Confernce on High-Power Lasers, **3264** 2-8 (1998).

[2] C. D. Orth, S. A. Payne, and W. F. Krupke, "A diode pumped solid state laser driver for inertial fusion energy," *Nuc. Fus.* **36**, 75-116, (1996).

[3] Randall J. St. Pierre et. al., 'Diode-array-pumped kilowatt laser', SPIE Proceedings Volume 3264 pp. 2-8 (1998).

[4] Aka G et. al. "Linear and nonlinear optical properties of GdCOB" JOSA B, **14** 2238-2247 (1997).

[5] Iwai M Kobayashi T, Furuya H, Mori Y., Sasaki T. "Growth and characterization of GdCOB and YCOB as new nonlinear optical materials " Japanese J. Applied Physics **36** 276-279 (1997).

[6]D. Eimerl "High Average Power Frequency Conversion" IEEE J. Quantum Electron. **23** 575-592 (1987).

Tunable Nonlinear Beam Defocusing in Infiltrated Photonic Crystal Fibers

Christian R. Rosberg[1], Francis H. Bennet[1], Dragomir N. Neshev[1], Per D. Rasmussen[2], Ole Bang[2], Wieslaw Krolikowski[1], Anders Bjarklev[2], and Yuri S. Kivshar[1]

[1] *Nonlinear Physics Centre and Laser Physics Centre, Centre for Ultrahigh-bandwidth Devices for Optical Systems (CUDOS), Research School of Physical Sciences and Engineering, Australian National University, Canberra ACT 0200, Australia*

[2] ***COM•DTU**, Technical University of Denmark, Ørsteds Plads 345V, DK-2800 Kgs. Lyngby, Denmark*

E-mail: crr124@rsphysse.anu.edu.au

We demonstrate a novel experimental platform for discrete nonlinear optics based on infiltrated photonic crystal fibers. We observe tunable discrete diffraction and nonlinear self-defocusing, and apply the effects to realize a compact all-optical power limiter.

OCIS codes: 190.4420, 190.5940

Nonlinear periodic photonic structures offer unique opportunities for manipulating the flow of light by exploiting the interplay between nonlinearity and periodicity[1]. While design options for one-dimensional periodic structures are inherently limited, two-dimensional structures open up the possibility of realizing a whole range of transverse geometries with different symmetries and unique properties. Only a few physical systems, however, have so far proved suitable for experimental studies of nonlinear wave propagation in two-dimensional periodic structures. These include photorefractive optically-induced lattices[2], fs-laser written waveguide arrays[3], and multicore optical fibers[4], each showing different advantages and limitations with respect to e.g. structural stability, tunability, and the access to observation of nonlinear effects. To fully explore the scientific and technological potential of periodic and nonlinear optical media, it is desirable to identify new experimental platforms that combine the advantages of high-quality fabricated structures with the attractiveness of tunability and strong nonlinear response.

Here we explore the use of infiltrated photonic crystal fibers (PCFs) for the study of discrete and nonlinear light propagation in extended two-dimensional periodic systems. Filling the hollow sections of PCFs with liquids allows for combining specific light guiding properties with strong material interactions for e.g. enhancement of nonlinear effects, optical sensing, and tunable devices[5,6]. In this work, we experimentally demonstrate strongly tunable beam diffraction in a triangular waveguide array created by infiltration of the cladding holes of a standard PCF with high index nonlinear liquid, and employ the thermal nonlinearity of the liquid to achieve beam self-defocusing at higher light intensity. Based on the observed effects we realize a compact all-optical power limiter device with tunable characteristics. Our use of commercially available fabricated microstructures in combination with liquid infiltration avoids the need for specialized high-precision fabrication procedures[4], and provides high tunability and nonlinearity at moderate laser powers while taking advantage of a simple and compact experimental setup.

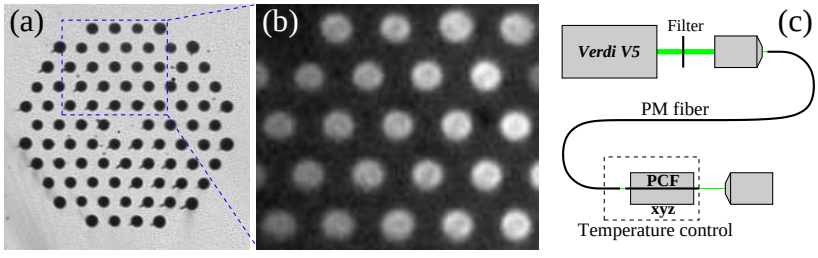

Fig. 1. Microscope images of (a) the photonic crystal fiber used in the experiment, and (b) section of fiber cladding after infiltration with a high index liquid. (c) Schematic of the experimental setup for coupling of light into the infiltrated PCF. PM – polarization maintaining fiber, xyz – 3 dimensional translational stage.

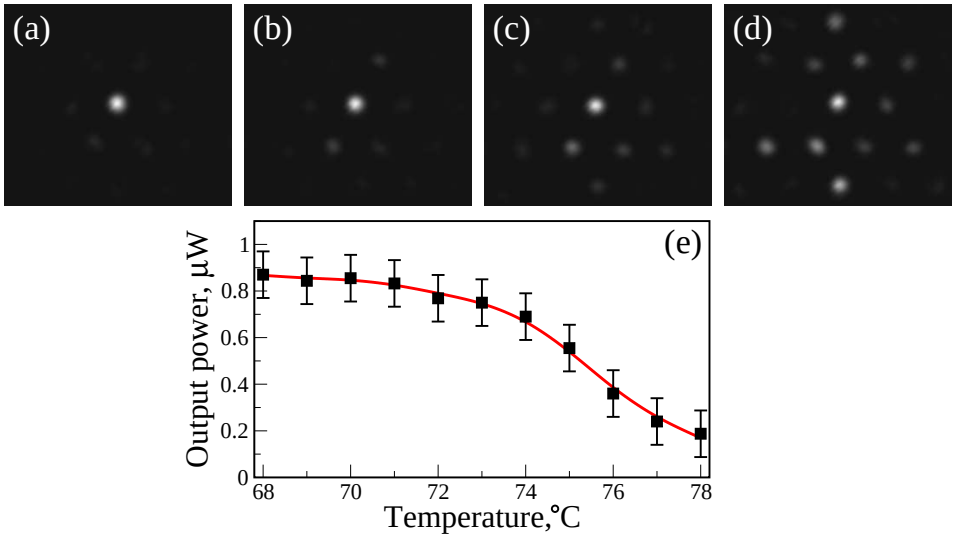

Fig. 2. (a-d) Linear output intensity distribution at temperature 72, 73, 74, and 75 °C, respectively. (e) Output power at the central lattice site measured as a function of temperature.

The experiment is performed in a 20 mm long piece of commercially available silica PCF (Crystal Fibre LMA-15), shown in Fig. 1(a). The cladding region consists of 84 air holes of diameter $d = 5\,\mu$m arranged around the fiber core in a triangular pattern with pitch $\Lambda = 10\,\mu$m. By use of capillary forces the air holes are filled with castor oil, which has a refractive index ($n = 1.48$) slightly higher than that of silica ($n = 1.46$). This results in the creation of a two-dimensional array of high index waveguides as shown in Fig. 1(b). The PCF sample is placed inside a temperature controlled oven (HC Photonics TC038) which can be stabilized to ± 0.1°C over a wide temperature range, allowing for thermo-optic tuning of the castor oil. Light from a Verdi-V5 continuous-wave laser ($\lambda = 532$ nm) is coupled into the central channel of the PCF waveguide array by use of a single-mode polarization maintaining (PM) fiber [Fig. 1(c)]. The mode field diameter of the PM fiber (Newport F-SPA) is 3.6 μm which provides a good match to the fundamental mode of the infiltrated waveguides. After propagation through the sample, the output beam is imaged by a microscope objective. Neutral density filters mounted between the laser and the PM fiber allow for controlling the beam power.

At room temperature the refractive index step between the glass and the infiltrated castor oil is $2 \cdot 10^{-2}$, and the cladding waveguides forming the triangular array shown in Fig. 1(b) are strongly multi-mode and decoupled from each other. By exploiting the large thermo-optic coefficient of the castor oil (measured to be $-3 \cdot 10^{-4}\mathrm{K}^{-1}$), it is possible to decrease the refractive index step to below $2 \cdot 10^{-3}$ by heating the fiber to above 70 °C. In this regime, the waveguides become single-mode, and the coupling between neighboring sites through evanescent mode field overlap is significantly increased. Figures 2(a-d) show the measured output intensity distribution for single site input excitation when the temperature is increased from 72 through 73, 74, and 75 °C, respectively. A considerable amount of light is seen to tunnel into the surrounding waveguides as the system is heated. The output pattern observed at 75 °C [Fig. 2(d)] features a central dominating peak while light in the neighboring waveguides form a lower intensity distribution resembling a hexagonal star. At higher temperatures the waveguide coupling is further increased, and as a result the strongly diffracting beam reaches the boundaries of the periodic structure [cf. Figs. 1(a) and 1(b)], and the triangular symmetry is broken. Apart from such boundary effects, small irregularities of the structure (due to nonuniform hole size and separation, or variations in the composition or infiltration of the waveguide liquid) are expected to significantly compromise symmetric diffraction and and lead to randomness- and disorder-related effects[4,7]. Indeed, even for beams confined within the periodic structure, some degree of disorder and coupling asymmetry is always observed in the experiment. Typical output profiles [Fig. 2(a-d)], however, resemble the discrete diffraction pattern predicted by theory and observed previously in triangular lattices[4].

The tunable beam diffraction can be used for dynamically controlling optical attenuation[5], as illustrated in Fig. 2(e) which shows the measured output transmitted through the central waveguide as a function of fiber temperature. The measurement was done by imaging the output beam onto a spatial filter blocking all but the central part of the beam.

Next we investigate how the thermal defocusing nonlinearity of castor oil affects beam propagation in the waveguide array. Because of the large and negative thermo-optic coefficient inherent to most liquids, heating produced by partial absorption of the propagating beam translates into a significant decrease of the refractive index at higher light intensity. Figures 3(a-d) show the measured output intensity distribution for increasing laser power, when the externally controlled fiber temperature is fixed at a level corresponding to weak linear coupling, in this case 74 °C. The

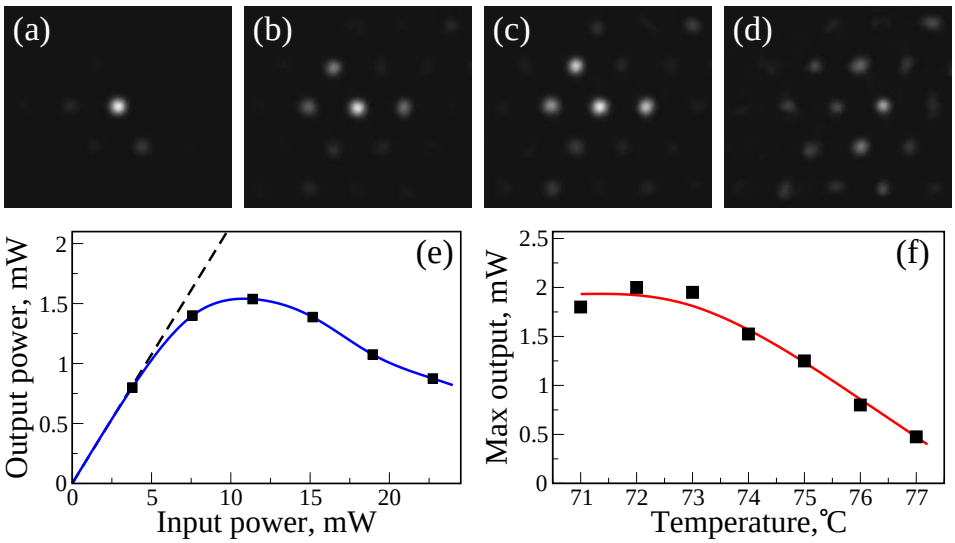

Fig. 3. (a-d) Output intensity distribution at 74 °C for increasing laser power; (a) corresponds to linear propagation. (e) Output power measured at the central lattice site versus input beam power at 74 °C. (f) Maximum output power in the nonlinear regime as a function of temperature.

first picture [Fig. 3(a)] corresponds to low power linear propagation. The thermal nonlinear response causes increased diffraction or *self-defocusing* of the probe beam, eventually spreading over most of the structure as the laser power is increased [Figs. 3(b-d)]. As a consequence, the output power in the central waveguide decreases relative to the input power, giving rise to a nonlinear power characteristic as shown in Fig. 3(e). At low laser power the dependence is linear, but above 5 mW input power the nonlinear defocusing increasingly limits the optical throughput, and the output power eventually drops after reaching a maximum at about 12 mW input power. Figure 3(f) shows how this nonlinear power characteristic can be combined with thermal control of the linear properties to externally tune the maximum output power in the nonlinear regime, thus realizing a tunable all-optical power limiter.

The strong defocusing observed in the experiment [Fig. 3] could indicate a high degree of nonlocality of the nonlinear response due to thermal diffusion, an idea supported by the fact that defocusing behavior is observed for any input position in the array. In disordered arrays a local nonlinear response, on the other hand, can lead to both localization and spreading, depending on the input position[7]. We believe that a characterization of the temporal dynamics of the system could shed further light on the possible effect of nonlocality, as e.g. transitory self-localization in the form of a nonlinear defect mode or discrete soliton[2] may happen on a short time scale before thermal equilibrium is reached.

In conclusion, we have demonstrated a novel experimental platform based on infiltrated PCFs for the study of discrete and nonlinear light propagation in two-dimensional periodic systems. We have experimentally demonstrated thermal control of linear diffraction and nonlinear self-defocusing in a triangular waveguide array, and realized tunable all-optical power limiting. The spatial control of light is enabled by the combined effects of discreteness, strong material tunability and nonlinearity, and does not rely on any architectural light guiding core defects as in the case of conventional PCF structures. We anticipate that the increasingly broad range of PCF structures available will stimulate further efforts in applying them in discrete nonlinear optics. The long propagation lengths that are accessible in fiber-based discrete systems could even allow for experimental studies of combined spatial and temporal nonlinear effects and thus pave the road for future demonstrations of spatiotemporal control of light.

References

1. D. N. Christodoulides, F. Lederer, and Y. Silberberg, Nature **424,** 817 (2003).
2. J. W. Fleischer, M. Segev, N. K. Efremidis, and D. N. Christodoulides, Nature **422,** 147 (2003).
3. T. Pertsch, U. Peschel, F. Lederer, J. Burghoff, M. Will, S. Nolte, and A. Tünnermann, Opt. Lett. **29,** 468 (2004).
4. U. Röpke, H. Bartelt, S. Unger, K. Schuster, and J. Kobelke, Opt. Express **15,** 6894 (2007).
5. B. J. Eggleton, C. Kerbage, P. S. Westbrook, R. S. Windeler, and A. Hale, Opt. Express **9,** 698 (2001).
6. T. T. Alkeskjold, J. Lægsgaard, A. Bjarklev, D. S. Hermann, A. Anawati, J. Broeng, J. Li, and S. T. Wu, Opt. Express **12,** 5857 (2004).
7. T. Pertsch, U. Peschel, J. Kobelke, K. Schuster, H. Bartelt, S. Nolte, A. Tünnermann, and F. Lederer, Phys. Rev Lett. **93,** 053901 (2004).

Multiwavelength kilowatt-peak-power light pulse source utilizing a picosecond diode laser for nonlinear bioimaging

H. Yokoyama[1], K. Takashima[1], M. Mure[2], H. C. Guo[1], J. Shikata[3], H. Ito[3], H. Tsubokawa[4], and N. Saito[5],

[1] New Industry Creation Hatchery Center (NICHe), Tohoku University

6-6-10 Aramaki-Aoba, Aoba-ku, Sendai 980-8579, Japan

[2] New Technology Research Laboratories, Sumitomo Osaka Cement Co., Ltd.

Toyotomi-cho 585, Funabashi-shi, Chiba 274-8601, Japan

[3] Research Institute of Electrical Communication (RIEC), Tohoku University

2-1-1 Katahira, Aoba-ku, Sendai 980-8577, Japan

[4] Graduate School of Information Sciences, Tohoku University

6-3-09 Aramaki-Aoba, Aoba-ku, Sendai 980-8579, Japan

[5] Biosignal Research Center, Kobe University,Rokkodai-cho 1-1, Nada-ku,Kobe 657-8501, Japan

yoko@niche.tohoku.ac.jp

Abstract: We generated octave-wide supercontinuum light with a diode-laser picosecond light source. The supercontinuum light was amplified to kilowatt peak-power levels by optical fiber amplifiers at three wavelength regions, and was successfully used for two-photon bioimaging.

OCIS codes: (140.5960) Semiconductor lasers; (190.2620) Frequency conversion; (320.7110) Ultrafast nonlinear optics; (170.2520) Fluorescence microscopy; (190.4180) Multiphoton processes; (320.5390) Picosecond phenomena.

1. Introduction

Supercontinuum (SC) light from visible wavelengths to the 1-μm region has attracted much attention as a novel physical phenomenon because it has become easy to generate using a nonlinear-optical photonic crystal fiber (PCF) and a femtosecond pulse Ti:sapphire laser [1,2]. Recent advances in SC light application have been extended to multiphoton bioimaging [3,4]. However, the common use of large-sized mode-locked solid-state lasers limits wide and practical applications of SC light. In this paper, we report an octave-wide SC light generation utilizing a low-average-power semiconductor laser picosecond pulse source. SC light pulses were amplified to kilowatt-peak-power levels at around 920, 980, and 1030 nm wavelength regions by optical fiber amplifiers which we developed, and amplified optical pulses were successfully applied for two-photon fluorescence imaging (TPI) of biological tissues such as mouse brain neurons containing green fluorescent protein (GFP). The present technology will enable various nonlinear bioimaging with compact and stable turn-key light pulse sources.

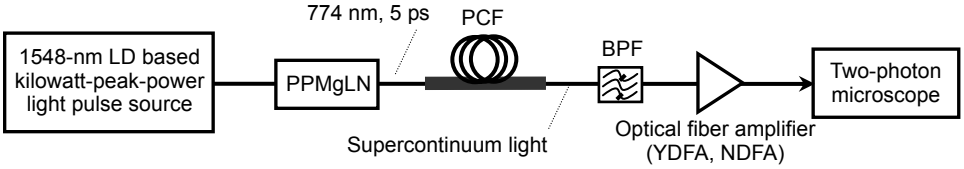

Fig.1. Schematic configuration of supercontinuum light generation utilizing a gain-switched laser diode (LD) based kilowatt-peak-power light pulse source. PPMgLN: periodically-poled MgO-doped $LiNbO_3$; PCF: photonic crystal fiber; BPF: band pass optical filter; YDFA: Yb-doped fiber amplifier; NDFA: Nd-doped fiber amplifier.

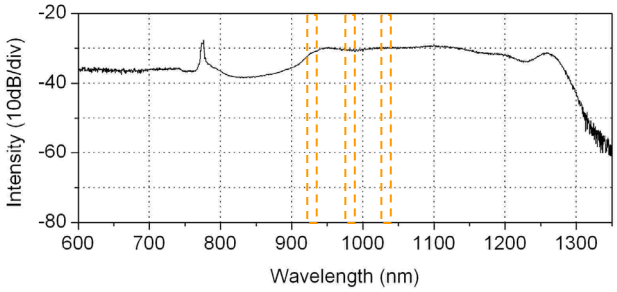

Fig.2. A typical optical spectrum for supercontinuum light generated from a photonic crystal fiber with 774-nm SHG light pulses. Broken-line-surrounded areas indicate the wavelength regions filtered and amplified.

2. Multiwavelength kilowatt-peak-power optical pulse source

Figure 1 presents a schematic diagram of our SC light pulse source. SC light was generated by a PCF from incident 774-nm light pulses with 1-kW peak power and 5-ps duration, The 774-nm light pulses were the second-harmonic (SH) output of amplified 1548-nm gain-switching semiconductor laser diode (LD), and the details of this light pulse source were described in References 5 and 6. An optical spectrum for octave-wide supercontinuum light was indicated in Fig.2. For TPI application, we extracted infrared light components using an approximately 10-nm-wide (FWHM) optical filter because we must keep the average optical power more than several tens of microwatt to amplify the filtered SC light to a power sufficient for TPI using an optical fiber amplifier. Note that we do not have to generate Fourier-transform-limited light pulses for TPI, and the measured pulse width was 1-2 ps. For 980 and 1030 nm light amplification, a laboratory-made Yb-doped fiber amplifier (YDFA) was used in which the active fiber length was approximately 1 m and all of the optical couplings were built using free-space optics geometry to remove coupling fibers. This YDFA configuration reduced the nonlinear spectral distortion during the amplification of light pulses to a kilowatt peak power level. The measured maximum output power of amplified light pulses was more than 40 mW in average excluding amplified spontaneous emission (ASE), and thus the peak power of the optical pulses was over 1 kW when the pulse repetition rate is 10 MHz. A similar procedure was adopted for generating high-peak-power 920-nm light pulses. In this case, however, light pulses were amplified with a Nd-doped fiber amplifier (NDFA). Since we found that the ASE in the present NDFA is more severe than the YDFA used, we increased the light pulse repetition rate to 50 MHz to reduce the ASE ratio.

3. Two-photon fluorescence bioimaging

For TPI, the amplified SC light pulses are directed into a two-photon fluorescence microscope that has been modified with a pair of galvanometer mirrors and a step motor for a three-dimensional scanning system [6]. Finally, the laser beam is focused by a 60× (1.2 NA) water-immersion objective onto a biological sample.

To test the feasibility of our light pulse source, a section of mouse kidney stained with Alexa Fluor 488 was used as the TPI specimen. The two-photon absorption range of Alexa Fluor 488 is very wide, from 800 nm to over 1 μm. Figure 3 (a) shows the TPI of the distal convoluted tubules and collecting tubules in the renal medulla using 1030-nm optical pulses at a 10-MHz repetition rate and 40-mW average power, indicating that clear high-resolution TPI is possible using our SC light source. Using 920 and 980 nm pulses also produced clear TPI for this specimen.

Next, we attempted to image fluorescent proteins in mouse brain neurons using TPI. Fluorescent proteins, such as green, yellow and red fluorescent protein (GFP, YFP, RFP), are widely used to label specific molecules in particular cell organelles both in vivo and in vitro. We examined the fluorescence of GFP, which is genetically bound to the protein kinase C (PKC) [7]. Although PKC is a key enzyme modulating neuronal functions, little is known concerning its location, and thus extensive TPI research works are expected at present.

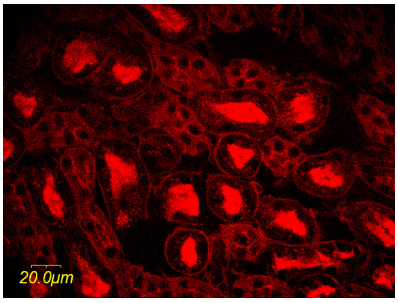

(a)

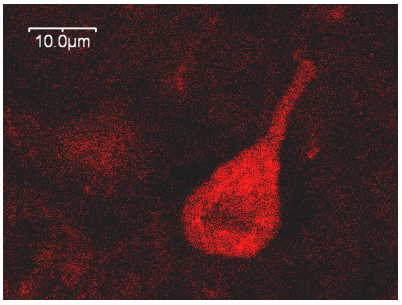

(b)

Fig.3. (a) TPI picture of mouse kidney tissues stained with Alexa Fluor 488 excited by amplified 1030-nm light pulses at 10-MHz repetition rate and 40-mW average power, and (b) TPI picture of the GFP bound to γ-type PKC in a mouse Purkinje neuron excited by amplified 920-nm light pulses at a 50-MHz repetition rate and 80-mW average power.

Figure 3 (b) shows the TPI of γ-type PKC in a mouse Purkinje neuron. At a 50-MHz repetition rate, and 80 mW average power, we detected GFP signals from the cell body. We found that γ-type PKC was distributed uniformly in the intracellular space around the cell body. We also confirmed the clear TPI of these neurons by using amplified 980 nm light pulses of 10-MHz and 40-mW average power. These results demonstrate that our SC light pulse source can provide a useful wavelength region for the TPI of GFP and redder fluorescent dyes.

4. Summary

In summary, we have generated octave-wide supercontinuum light using a compact and stable semiconductor laser picosecond light pulse source, then filtered and amplified to kilowatt peak power levels at wavelengths around 920, 980, and 1030 nm. Especially, the light pulses of 920 and 980 nm wavelengths were effective for the two-photon excitation of bio-specimens containing GFP. Note that our scheme is applicable to other light wavelengths within a generated supercontinuum bandwidth as long as we can create a proper optical amplifier. Therefore, our light source will be applicable for many multiphoton bioimaging methods, including two- or three-photon fluorescence, second- or third-harmonic generation, and coherent anti-Stokes Raman scattering.

5. References

1. J. Herrmann, U. Griebner, N. Zhavoronkov, A. Husakou, D. Nickel, J. C. Knight, W. J. Wadsworth, P. St. J. Russell, and G. Korn, "Experimental evidence for supercontinuum generation by fission of higher-order solitons in phonic fibers," Phys. Rev. Lett. **88**, 173901 (2002).
2. S. Coen, A. H. L. Chau, R. Leonhardt, J. D. Harvey, J. C. Knight, W. J. Wadsworth, and P. St. J. Russell "Supercontinuum generation by stimulated Raman scattering and paprametric four-wave mixing in photonic crystal fibers," J. Opt. Soc. Am. B **19**, 753-764 (2002).
3. H. N. Paulsen, K. M. Hilligse, J. Thgersen, S. R. Keiding, and J. J. Larsen, "Coherent anti-Stokes Raman scattering microscopy with a photonic crystal fiber based light source," Opt. Lett. **28**, 1123-1125 (2003).
4. K. Isobe, W. Watanabe, S. Matsunaga, T. Higashi, K. Fukui and K. Itoh, "Multi-spectral two-photon excited fluorescence microscopy using supercontinuum light source," Jpn. J. Appl. Phys. **44**, L167-169 (2005).
5. T. Yoda, H. Yokoyama, K. Sato, H. Taniguchi, and H. Ito, "High-peak-power picosecond optical-pulse generation with a gain-switched semiconductor laser, and high-efficiency wavelength conversion," in *the Pacific Rim Conference on Lasers and Electro-Optics (CLEO-PR)*, CFM2-5, Tokyo, Japan, July 2005.
6. H. Yokoyama, H. C. Guo, T. Yoda, K. Takashima, K. Sato, H. Taniguchi, and H. Ito, "Two-photon bioimaging with picosecond optical pulses from a semiconductor laser," Opt. Express **14**, 3467-3471 (2006).
7. C. Tanaka, and Y. Nishizuka, "The protein kinase C family for neuronal signaling," Ann. Rev. Neurosci. **17**, 551-567 (1994).

Inhomogeneous Tensorial Nonlinear Responses from an Array of Gold Nanoparticles

Martti Kauranen, Hannu Husu, and Brian K. Canfield
Institute of Physics, Optics Laboratory, Tampere University of Technology, P. O. Box 692, FI-33101 Tampere, Finland
martti.kauranen@tut.fi

Juha Kontio, Jukka Viheriälä, Tuomo Rytkönen, and Tapio Niemi
Optoelectronics Research Center, Tampere University of Technology, P. O. Box 692, FI-33101 Tampere, Finland

Eric Chandler, Alex Hrin, and Jeff A. Squier
MOABC, Department of Physics, Colorado School of Mines, 1523 Illinois St., Golden, CO 80401

Abstract: We use second- and third-harmonic-generation microscopy to address nonlinear responses of individual gold nanoparticles in an array. Widely-variable, polarization-dependent responses of individual particles indicate tensorial inhomogeneities in the sample.

OCIS codes: (190.0190) Nonlinear optics; (260.3910) Metals, optics of

Metal nanostructures have attractive applications in nanoscale lensing [1], optical antennae [2], and magnetic metamaterials [3]. In the metamaterial way of thinking, an individual nanoparticle is an artificial atom whose properties can be designed at will, and their collection acts as a medium with effective properties. However, the plasmonic and magnetic resonances of individual particles depend sensitively on their size, shape, and environment. Present nanofabrication techniques result in structures that contain unintended, small-scale features, such as random defects, which can lead to inhomogeneous effects (differences between individual particles). Such small features may act as attractors for strong local fields and thus substantially influence nonlinear responses that scale with a high power of the field. The nonlinear response of an individual particle therefore depends on a complicated interplay between: 1) plasmonic resonances and 2) resultant local field distributions, both controllable through design, and also 3) uncontrollable defects. The relative importance of these factors may differ for even-order processes, which have a strong noncentrosymmetry requirement and sensitivity to symmetry-breaking defects, and odd-order processes, which are less sensitive to symmetry. In order to understand the relative importance of these factors, it is important to examine various nonlinear responses of individual nanoparticles.

In this Paper we use second- and third-harmonic-generation (SHG and THG, respectively) microscopy of arrays of gold nanoparticles to address nonlinear responses of individual particles. The results show that responses vary widely from particle to particle and exhibit strong dependences on the polarizations of both the fundamental and signal beams. This result indicates differences in the level and details of symmetry breaking of individual particles, leading to robust nonlinear activity from them for different polarization combinations. Whereas this can be expected for SHG, which is sensitive to symmetry breaking of individual particles, it is surprising for THG, which is less sensitive to symmetry. This suggests that even the third-order response may be dominated by the defects in individual particles, possibly through field localization at small-scale features.

Cylindrical gold nanoparticles (‘nanodots’) were fabricated through nanoimprint lithography (NIL). Regular arrays of nanodots with diameters of 250 nm were fabricated with spacings of 400, 500, 1000, 1500, and 2000 nm, where the larger spacings allowing individual particles to be addressed. A scanning electron micrograph (SEM) of one nanodot array is shown in Fig. 1(a). Linear extinction spectra for the samples were measured using a white light source and fiber optic spectrometers covering the range of 400–1650 nm. The nanodot arrays exhibited no dichroism, as seen in Fig. 1(b). Only one extinction resonance peak is observed, indicating that on average the arrays are highly symmetric along both array axes shown in Fig. 1(a).

Nonlinear optical microscopy was performed using a Nd:glass fs laser beam (fundamental wavelength 1064 nm, pulse length 120 fs, average power 50 mW). X-Y scanning was accomplished by two orthogonally oriented scan mirrors on voltage-driven rotation stages that directed the beam into a high numerical aperture (NA = 0.65) microscope objective focused on the NIL array. In transmission, the generated harmonic was recollimated with a second objective, passed through a polarizer, fundamental-blocking filter, and interference filter before being detected by a photomultiplier tube (PMT). In epi-configuration, an appropriate harmonic separator (dichroic mirror) was inserted prior to the objective. The generated epi-harmonic was thus reflected by the harmonic separator into a

similar detection arm. A major advantage of epi-configuration, however, is that a lossy interference filter is not needed before the PMT, thereby substantially increasing the harmonic intensity at the detector and improving the signal-to-noise ratio in the scans.

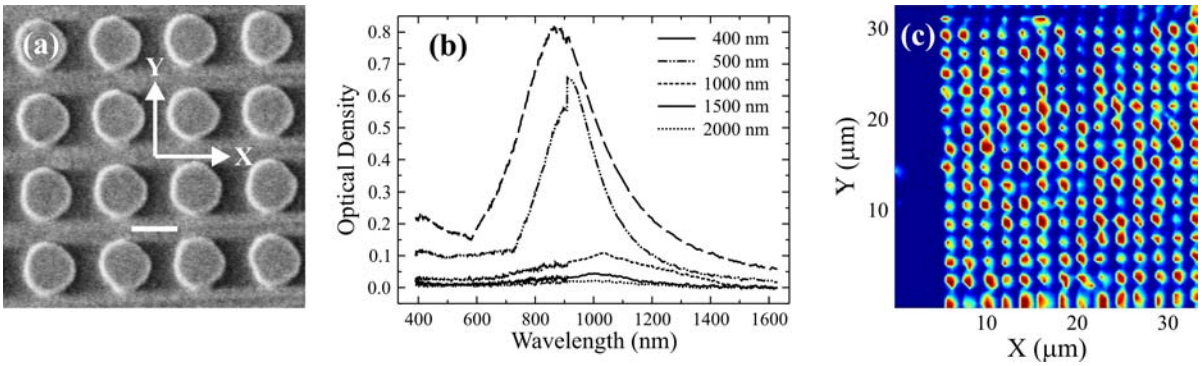

Fig. 1. NIL-fabricated gold nanodots. (a) SEM of 250 nm diameter nanodots with 400 nm spacing (scale bar is 250 nm); (b) unpolarized linear extinction spectra for different array spacings; (c) example of transmitted SHG for a 300 nm nanodot array with 2000 nm spacing using unpolarized detection. The array's edge is clearly visible on the left side.

An example transmission SHG scan of a nanodot array using unpolarized detection is shown in Fig. 1(c). The regular structure of the array is readily apparent, and the array's edge is clearly seen on the left side of the scan, indicating good contrast between substrate and nanodots. However, the THG scans in transmission were poor at best. Much higher harmonic signal and lower background was achieved in epi-configuration without the interference filter.

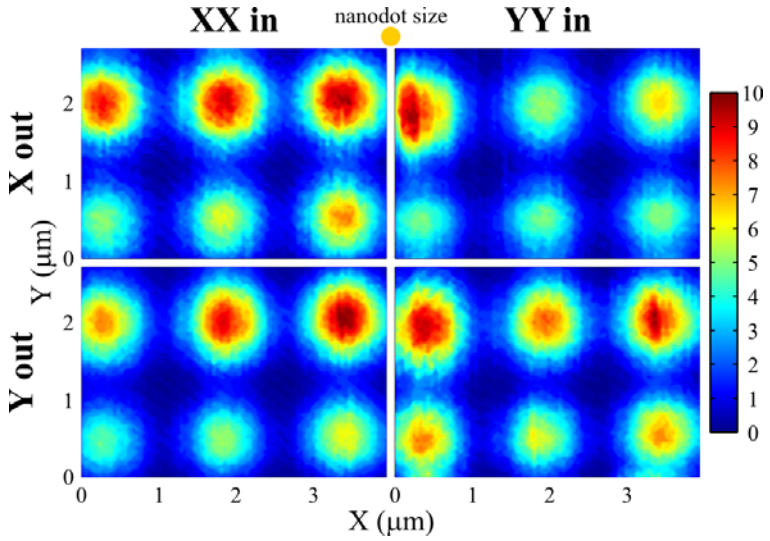

Fig. 2. Polarized epi-SHG responses of 250 nm diameter nanodots with 1500 nm spacing for the polarizations indicated. Note that in each plot the background has been subtracted and the plot separately normalized to its maximum value.

Polarized epi-SHG scans are shown in Fig. 2 for nanodots 250 nm in diameter with 1500 nm spacing. This particular array was chosen to provide cleanly-separated nanodots. The active response areas appear much larger than the actual nanodot size due to the convolution of the relatively large gaussian focal spot (spot diameter ~ 2 μm) interacting with the smaller nanodot (shown at the top of the figure).

As Fig. 2 shows, there are clearly strong polarization dependences from nanodot to nanodot. This is to be expected for SHG, which is extremely sensitive to symmetry, from nanodots possessing small defects. An ideal nanodot would be centrosymmetric and therefore should yield no SHG at normal incidence [4]. The plots in Fig. 2 indicate that the nanodots deviate from ideal, rendering them SHG-active. The differences between individual nanodots demonstrate that these symmetry-breaking features are distributed randomly throughout the array.

Fig. 3 displays the polarized epi-THG responses for the same set of nanodots. Surprisingly, the THG scans also reveal strong polarization dependences, even though THG should be less sensitive to symmetry. In addition, although the mixed polarization components XYYY and YXXX are disallowed by symmetry in isotropic media [4], the nanodots exhibit significant responses for these combinations. On the other hand, the responses XXXX and YYYY should be indistinguishable for ideal nanodots, but there are clear differences between them in Fig. 3. These results are again indicative of small symmetry-breaking features driving the nonlinear responses of the nanodots.

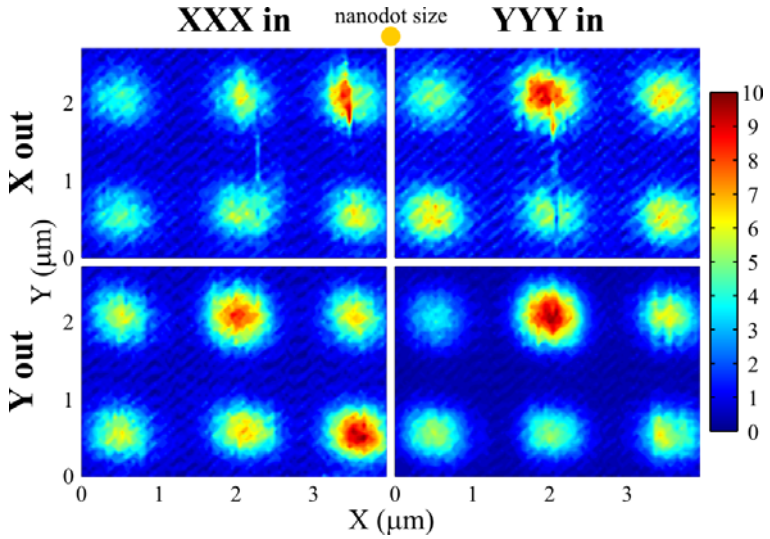

Fig. 3. Polarized epi-THG responses from the same nanodots as in Fig. 2 for the polarizations indicated. The background has again been subtracted and each plot separately normalized to its maximum value.

To conclude, we have employed nonlinear optical microscopy to investigate polarization-dependent nonlinear responses of individual gold nanoparticles. The responses were found to vary widely between nanodots. The detection of such varying, symmetry-forbidden nonlinear responses indicates that small-scale, symmetry-breaking features are randomly distributed throughout the arrays. The nonlinear responses are therefore dominated by these small features through the strongly localized fields in their vicinity. This microscopy method also suggests a viable, rapid means of characterizing the quality of the particles over the entire array scale.

References

1. A. Sundaramurthy, P. J. Schuck, N. R. Conley, D. P. Fromm, G. S. Kino, and W. E. Moerner, "Toward Nanometer-Scale Optical Photolithography: Utilizing the Near-Field of Bowtie Optical Nanoantennas," Nano Lett. **6**, 355–360 (2006).
2. P. Mühlschlegel, H.-J. Eisler, O. J. F. Martin, B. Hecht, and D. W. Pohl, "Resonant Optical Antennas," Science **308**, 1607–1609 (2005).
3. C. Enkrich, M. Wegener, S. Linden, S. Burger, L. Zschiedrich, F. Schmidt, J. F. Zhou, T. Koschny, and C. M. Soukoulis, "Magnetic Metamaterials at Telecommunication and Visible Frequencies," Phys. Rev. Lett. **95**, 203901 (2005).
3. B. K. Canfield, S. Kujala, K. Laiho, K. Jefimovs, T. Vallius, J. Turunen, and M. Kauranen, "Linear and nonlinear optical properties of gold nanoparticles with broken symmetry," J. Nonlinear Opt. Phys. Mat. **15**, 43 (2005).
4. R. W. Boyd, *Nonlinear Optics* (Academic Press, San Diego, 1992).

Chirped Biphotons Using Quasi Phase Matching

S. Sensarn and S. E. Harris
Edward L. Ginzton Laboratory, Stanford University, Stanford, California 94305
sensarn@stanford.edu

We describe techniques for numerically simulating broadband, time-energy entangled biphoton generation by spontaneous parametric down conversion in quasi-phase-matched nonlinear crystals. Typical domain errors have negligible effect on the phase spectrum of the biphoton wavefunction.

OCIS codes: (270.0270) Quantum Optics; (190.0190) Nonlinear Optics

1. Introduction

Spontaneous parametric down conversion (SPDC) is a second-order nonlinear optical process in which a pump photon is converted into two lower-energy photons (a biphoton pair consisting of a signal and an idler photon) in a nonlinear crystal. The signal and idler photons are time-energy entangled in that they conserve the energy of the pump photon and are generated at the same location inside the crystal (and hence arrive at two detectors with correlated timing). Knowing the arrival time or energy of the signal photon gives information about the arrival time or energy of the idler photon, and vice versa. These entangled photons find application in fields such as quantum communications, quantum tomography, and nonlinear optics [1-3].

Recent literature has suggested the use of quasi-phase-matched (QPM) nonlinear crystals to generate chirped biphotons [4]. In particular, when the instantaneous wavevector of the poled grating varies linearly across the length of the crystal, the biphoton wavefunction takes analytic form, and effects such as non-local compression of the wavefunction and quantum enhancement in nonlinear optics can be presented mathematically. However, real QPM crystals have imperfect domain structure and can exhibit random perturbations in domain edge position as large as 30% of the domain width. This poster describes methods for numerically computing the biphoton wavefunction in realistic crystals and shows that typical random errors in domain edge position distort the signal and idler amplitude spectra but have little effect on the phase spectrum.

2. Chirped Biphoton Generation

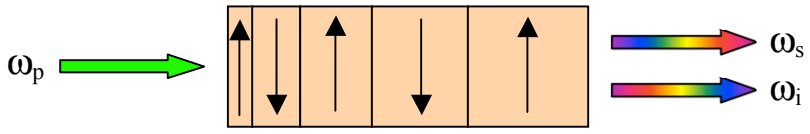

Fig. 1. Chirped biphoton generation using a chirped grating inside a nonlinear crystal.

Figure 1 shows a QPM nonlinear crystal in which the grating wavevector (which phase matches collinear generation of signal and idler fields) varies linearly with crystal length. The resultant signal and idler fields have larger bandwidths than the equivalent fields generated by a non-chirped crystal and exhibit chirped temporal waveforms. If group velocity dispersion can be neglected, and parametric gain is approximately constant for all frequencies, the signal and idler fields will have ideal linearly-chirped waveforms. One may show that the biphoton wavefunction also has such a chirped profile [4].

For a realistic example, we consider lithium niobate as a nonlinear crystal and examine type I, non-degenerate, collinear biphoton generation in the plane wave approximation. In this calculation, all waves are polarized along the extraordinary axis, and we use a 532 nm pump wavelength. The 1 cm long crystal grating is chirped to phase match a 442 nm signal bandwidth centered at 765 nm, where the signal is defined as the photons whose wavelengths are shorter than the degenerate wavelength (1064 nm). The direction of the chirp is that which phase matches blue signal photons on the input edge of the crystal and red signal photons on the output edge of the crystal. The generated power spectral density (PSD) of the signal and the phase spectrum of the biphoton wavefunction are shown in Fig. 2. The PSD is not flat due to the frequency dependence of the parametric gain, which is included in the calculation. The phase spectrum contains all information about broadening or compression of the wavefunction. The PSD and phase spectrum are calculated by numerically integrating the differential equations governing the

growth of the signal and idler field operators. The sign of the nonlinear coefficient is appropriately reversed at each poled domain edge, allowing perturbations of edge positon (poling errors) to be studied.

To examine the effects of poling errors in a real crystal, we consider the capabilities of current poling technology. If the poling is performed using electric fields, the mask sets the nominal position of each domain edge. Imperfections in the poling process then perturb these edges about their designed positions.

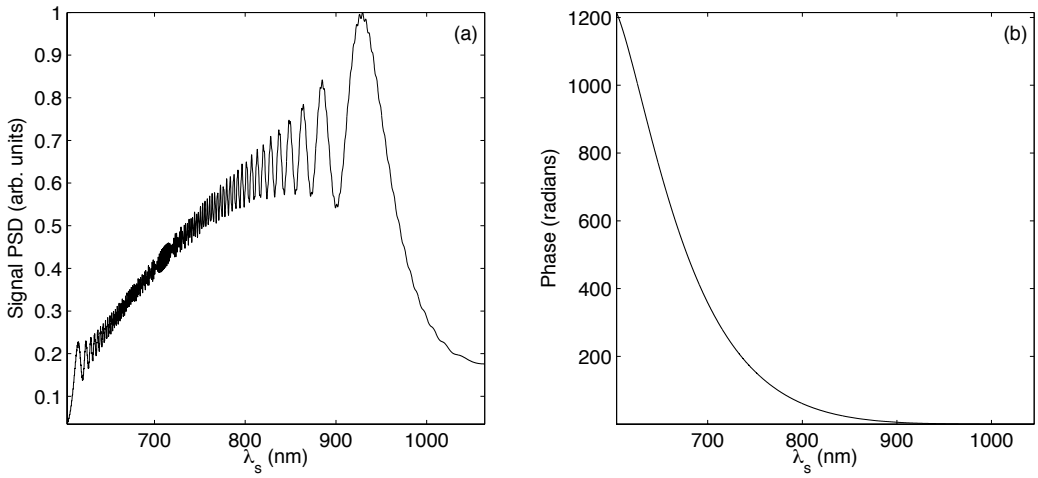

Fig. 2. (a) Signal power spectral density and (b) phase spectrum of the biphoton wavefunction for a chirped crystal with ideal poling. The idler PSD is the mirror reflection of the signal PSD about the degenerate frequency.

In this analysis, we assume normally-distributed random errors in domain edge position. In choosing the magnitude of such errors, we note that, for a periodically-poled crystal, a standard deviation equal to 37.5% of the domain width corresponds to a 50% drop in effective nonlinearity [5]. Current poling technology is capable of achieving at least 50% of ideal conversion efficiency in second harmonic generation (SHG) producing 532 nm light, corresponding to poling errors less than 37.5% of the domain width. This means that it is reasonable to expect current poling technology to exhibit errors in domain edge position with standard deviations less than 37.5% of about 3.5 μm (the domain width that phase matches SHG of 532 nm light in lithium niobate). We use a standard deviation of 1.31 μm in this analysis.

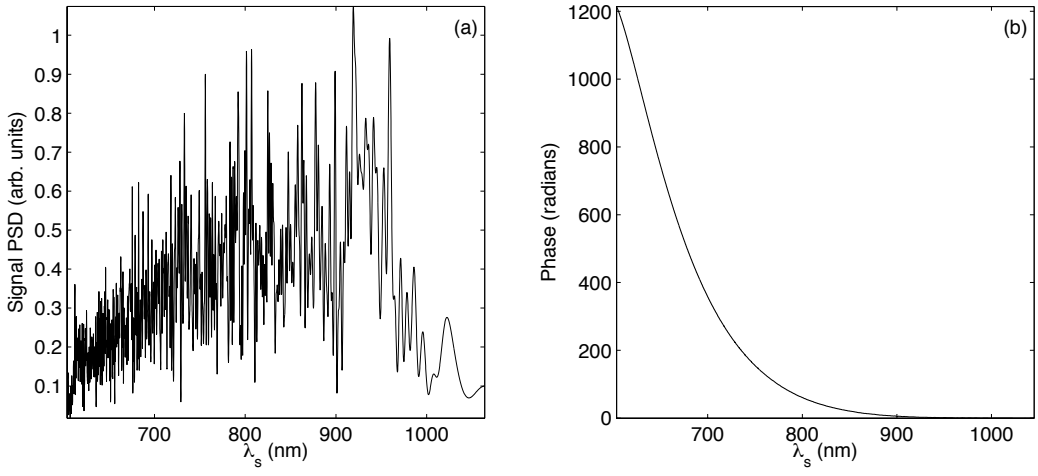

Fig. 3. (a) Signal power spectral density and (b) phase spectrum of the biphoton wavefunction for an identical crystal as in Fig. 2, except with typical errors in domain edge position. PSD plot is normalized by the same constant used to normalize Fig. 2(a).

Figure 3 shows the generated PSD and phase spectrum for the crystal with poling errors. The PSD is strongly distorted, but the phase spectrum is nominally unaffected by the poling errors. To analyze the effect of poling error on phase, the phase spectra from Fig. 2(b) and Fig. 3(b) are subtracted. With the mean removed, the resulting phase error and distribution are shown in Fig. 5. The standard deviation of the phase spectrum error is 0.250 radians,

meaning that, with the correct choice of (arbitrary) global phase, 68% of the phase spectrum will deviate from the ideal spectrum by less than 0.250 radians. This phase error should have negligible effect on the temporal correlation width of the biphoton.

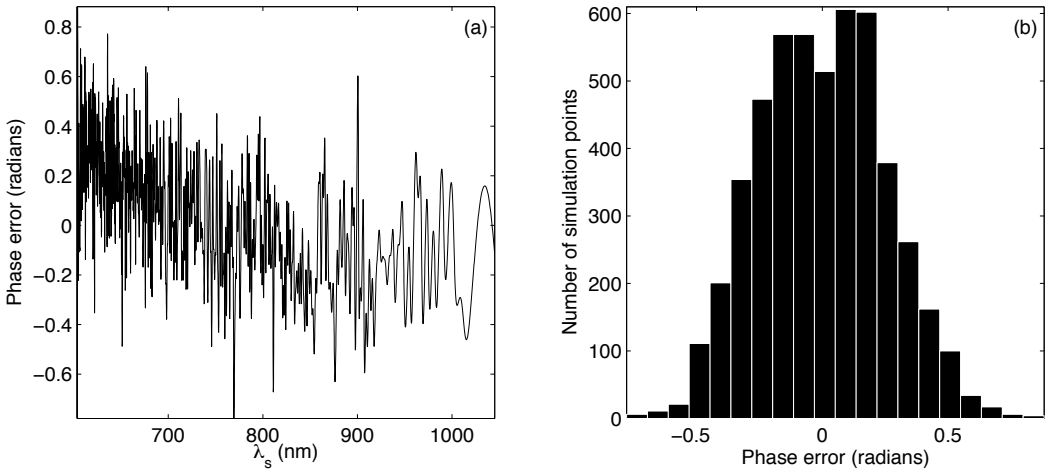

Fig. 5. Phase spectrum error and distribution. The phase error is calculated by subtracting the phase spectrum generated by the crystal with domain errors from the spectrum generated by the ideal crystal. The mean is subtracted to center the distribution at zero phase error (this is simply a choice of arbitrary global phase). The standard deviation of the phase error distribution is 0.250 radians.

3. Summary

We describe a method for generating broadband biphotons using chirped QPM nonlinear crystals show that numerical simulations predict a negligible effect of typical domain edge position poling errors on the phase spectrum of the biphoton wavefunction.

4. References

[1] W. Tittel, J. Brendel, H. Zbinden, and N. Gisin, "Quantum Cryptography Using Entangled Photons in Energy-Time Bell States," Phys. Rev. Lett. **84**, 4737 (2000).

[2] Magued B. Nasr, Bahaa E. A. Saleh, Alexander V. Sergienko, and Malvin C. Teich, "Demonstration of Dispersion-Canceled Quantum-Optical Coherence Tomography," Phys. Rev. Lett. **91**, 083601 (2003).

[3] Barak Dayan, Avi Pe`er, Asher A. Friesem, and Yaron Silberberg, "Nonlinear Interactions with an Ultrahigh Flux of Broadband Entangled Photons," Phys. Rev. Lett. **94**, 043602 (2005).

[4] S. E. Harris, "Chirp and Compress: Toward Single-Cycle Biphotons," Phys. Rev. Lett. **98**, 063602 (2007).

[5] Martin M. Fejer, G. A. Magel, Dieter H. Jundt, and Robert L. Byer, "Quasi-Phase-Matched Second Harmonic Generation: Tuning and Tolerances," IEEE J. Quantum Electron. **28**, 2631 (1992).

Key to Authors and Presider

(BOLD denotes presenting author)